26TH ANNUAL MEETING

Friday,
October 20th, 2017

Sheraton Boston Hotel
39 Dalton St.,
Boston, MA 02199

International Society For Anaesthetic Pharmacology 2017 Syllabus

6737 W. Washington St., Suite 4210 • Milwaukee, WI 53214
(p) 414-755-6296 • (f) 414-276-7704 • www.isaponline.org • isaphq@isaponline.org

Mission Statement

The **International Society for Anaesthetic Pharmacology (ISAP)** is a nonprofit organization with an international membership, which is dedicated to teaching and research about clinical pharmacology in anesthesia, with particular reference to anesthetic drugs.

Accreditation Information

Target Audience
This program is designed for an international audience of general anesthesiologists, pharmacological anesthesiologists, technology anesthesiologists and specialty physicians.

Learning Objectives:
The overall purpose of this activity is to enable the learner to:

1. Understand how to optimize perioperative pain management to reduce chronic opioid use and prevent or treat hypoventilation, including potential future approaches.
2. Comprehend general anesthesia's long-term impact on cognitive function and be prepared to discuss this risk with patients.
3. Appreciate how to improve reproducibility in biomedical research.

Practice Gaps:

- Opioid use disorder has been identified as a national epidemic. Anesthesiologists' perioperative management may influence long-term opioid use by patients.
- Reducing the health and societal consequences of opioid use requires identification of effective alternative approaches to pain management.
- Opioids and other anesthetic drugs impair respiration through several mechanisms, putting patients at risk for hypoxia and irreversible organ damage.
- An alarmingly high fraction of biomedical research study results cannot be replicated.
- General anesthetic drugs may produce long-term cognitive effects on very young or old patients.

Accreditation Statement:
This activity has been planned and implemented in accordance with the accreditation requirements and policies of the Accreditation Council for Continuing Medical Education (ACCME) through the joint providership of Amedco and the International Society of Anaesthetic Pharmacology (ISAP). Amedco is accredited by the ACCME to provide continuing medical education for physicians.

Credit Designation Statement:
Amedco designates this live activity for a maximum of *6.75 AMA PRA Category 1 Credits*™. Physicians should claim only the credit commensurate with the extent of their participation in the activity.

Continuing Medical Education (CME) Certificate

IMPORTANT!
The online certificate site will be available from October 21st to November 21st. **After that date, the site will be removed and certificates will no longer be available.** If you need a CME certificate, you must complete the evaluation and certificate process prior to that date; otherwise you will forfeit your credit for the course.

To get your certificate, just go to ISAP.cmecertificateonline.com.

1. Go to **ISAP.cmecertificateonline.com.**
2. Click on the **"26th Annual Meeting"** link. On the site, you will be asked to evaluate various aspects of the program. You may then print your certificate.

Please address any questions about the process to: Certificate@AmedcoEmail.com.

Planning Committee
Michael J. Avram, PhD
Northwestern University
Feinberg School of Medicine
Chicago, IL USA

Stuart A. Forman, MD, PhD
Massachusetts General Hospital
Boston, MA USA

Faculty
David J. Clark, MD, PhD
Stanford University
Stanford, CA USA

Joseph Cotten, MD, PhD
Massachusetts General Hospital
Boston, MA USA

Deborah J. Culley, MD
Brigham and Women's Hospital
Boston, MA USA

Albert Dahan, MD, PhD
Leiden University Medical Center
Leiden, Netherlands

Andrew Davidson, MBBS, MS, FANZCA
University of Melbourne
Victoria, Australia

Tong J. Gan, MD, MHS, FRCA
Stony Brook University
Stony Brook, NY USA

Padma Gulur, MD
Duke University School of Medicine
Durham, NC USA

Timothy T. Houle, PhD
Massachusetts General Hospital
Boston, MA USA

Evan D. Kharasch, MD, PhD
Washington University School of Medicine in St. Louis
St. Louis, MO USA

Jianren Mao, MD, PhD
Massachusetts General Hospital
Boston, MA USA

Mohamed Naguib, MD
Cleveland Clinic
Cleveland, OH USA

Yan Xu, PhD
University of Pittsburgh
Pittsburgh, PA USA

26th Annual Meeting Agenda

07:00 – 08:00	**Breakfast (Sponsored) & Registration**
08:00 – 08:10	**Welcome** ISAP President, Mohamed Naguib, MD
08:10 – 08:15	**Introduction to the Program** Michael J. Avram, PhD and Stuart A. Forman, MD, PhD
08:15 – 09:00	**Session 1 – The Opioid Epidemic**
08:15 – 08:35	**Opioid Analgesics – The Good, The Bad, and The Ugly** Jianren Mao, MD, PhD
08:35 – 08:55	**Perioperative Pain Management of Opioid-Tolerant Patients** Padma Gulur, MD
09:00 – 09:30	**Break**
09:30 – 10:30	**Session 2 – Respiratory Stimulants to Treat Anesthetic-induced or Opioid-induced Hypoventilation**
09:30 – 10:00	**Mechanisms of Drug-Induced Respiratory Depression** Albert Dahan, MD, PhD
10:00 – 10:30	**Developing Drugs to Treat Respiratory Depression - Translational Studies** Joseph Cotten, MD, PhD
10:30 – 11:30	**Session 3 – New Pharmacological Approaches to Post-op and Chronic Pain**
10:30 – 11:00	**Novel Opiod Agonists** Tong J. Gan, MD, MHS, FRCA
11:00 – 11:30	**RELIEPH as Potential Pain Modulatory Therapy** Yan Xu, PhD
11:30 – 12:45	**Lunch, Business Meeting & Poster Session**
12:45 – 13:45	**Moderated Poster Discussion**
13:45 – 14:45	**Session 4 – Problems with Preclinical Research – Models, Design, Analysis, and Interpretation**
13:45 – 14:15	**Animal Models and Translational Pain Research** David J. Clark, MD, PhD
14:15 – 14:45	**Statistical Problems with Preclinical Research and How to Fix Them** Timothy T. Houle, PhD (MGH)
14:45 – 15:15	**Break**
15:15 – 16:15	**Session 5 – Neurotoxicity at Extremes of Age**
15:15 - 15:45	**The Use of General Anesthetics and Sedation Drugs in Young Children and Pregnant Women** Andrew Davidson, MBBS, MD, FANZCA
15:45 - 16:15	**POCD: What is it and Do the Anesthetics Play a Role** Deborah J. Culley, MD
16:15 – 16:55	**Keynote Speaker & Lifetime Achievement Award Winner:** Evan D. Kharasch, MD, PhD
16:55 – 17:00	**Closing Remarks**
17:00 – 18:00	**President's Reception**

Participant Notification

All people with control of the CME content for this activity (e.g., faculty/speakers, planners, abstract reviewers, moderators, authors, co-authors and administrative staff participating) disclosed their financial relationships to Amedco as shown in the list below, which also indicates the resolution, if applicable.

We acknowledge the potential presence of limitations on information, including, but not limited to: data that represents ongoing research; interim analysis; preliminary data; unsupported opinion; or approaches to care that, while supported by some research studies, do not represent the only opinion or approach to care supported by research.

Abstract Table of Contents

Commercial Support Levels

Platinum Plus

Baxter

www.baxter.com

Platinum

Masimo®

www.masimo.com

Entrepreneuer Silver

QM Quantium Medical

www.quantummedical.net

Novel Opioid Paradigms: Long-Duration Opioid for Same-Day Outpatient Surgery

Authors: Helga Komen, Jane Blood, L Michael Brunt[1], Evan D Kharasch
Department of Anesthesiology, Washington University School of Medicine, Saint Louis, MO
[1] Department of Surgery, Washington University School of Medicine, Saint Louis, MO

Background: More than 50 million Americans undergo outpatient surgery annually. Many report inadequate postoperative analgesia, and chronic postsurgical pain. Another problem is the reservoir of unused postoperative opioids due to overprescription. Typically, short-duration opioids are used for outpatient surgery. For inpatient surgery a single intraoperative dose of a long-duration opioid (i.e. methadone) produces better analgesia than repeated doses of short-duration opioids. However, the clinical effectiveness of long-duration opioids like methadone in outpatient surgery is not known. This investigation tested the hypothesis that in outpatient surgery intraoperative methadone compared with conventional short-duration opioids reduces postoperative opioid consumption and pain, with similar or diminished side effects.

Methods: Patients undergoing same day discharge surgical procedures (e.g. laparoscopic cholecystectomy) (n=60) were randomized 2:1 to receive either single-dose IV methadone at anesthesia induction (0.1 mg/kg or 0.15 mg/kg, ideal body weight) or short-duration opioid (controls: hydromorphone, fentanyl at practitioners' discretion) in a dose-escalation protocol. Intraoperative and postoperative opioid consumption (until discharge) was recorded and expressed in morphine equivalents. Patient pain intensity (at rest, with coughing, with activity) and sedation were assessed at 15, 30, 45 min, 1, 2, 3, 4 h after admission in the PACU and at discharge. Opioid side effects (Opioid-Related Symptom Distress Scale, ORSDS) and ventilatory depression (respiratory rate, oxygen saturation, re-intubation) were also assessed. After discharge, patients were given home diaries where they recorded daily pain, opioid use, and side effects, until postoperative day 30.

Results: Intraoperative methadone doses (mean ± SD) were 6 ± 1 mg (0.1 mg/kg) and 9 ± 1 mg (0.15 mg/kg). Average intraoperative total nonmethadone short-duration opioid use (morphine equivalents) was 25.5, 1.3 and 0.16 mg respectively (n=21, 18, 21) in control, 0.1mg/kg methadone and 0.15mg/kg methadone groups. Patients receiving a single 0.15 mg/kg methadone dose required significantly less opioid vs controls in the PACU (2 ± 3 vs 8±7 mg) and postoperatively during hospital stay (4 ± 4 vs 9±7 mg). Patients receiving intraoperative methadone (0.15 mg/kg) used less take-home opioids (total 30d IV morphine equivalents were 22± 2 mg after 0.15 mg/kg methadone vs 30 ± 1 mg in controls), and stopped taking opioids earlier. Patients receiving 0.15 mg/kg intraop methadone had lower pain scores on arrival in PACU compared to controls (numerical rating scale 3 ± 1 vs 5 ± 1.2). Pain scores at rest in the 30 day postoperative period were lower in patients receiving 0.15 mg/kg intraop methadone compared to controls (summed numerical rating scores were 10 ± 2 vs 23 ± 3). Sedation and adverse events were similar in patients receiving methadone and short-duration opioids intraoperatively.

Conclusion: A single intraoperative methadone dose (0.15 mg/kg ideal body weight) decreased intraoperative and postoperative opioid requirements and provided better analgesia, with similar side effects compared to patients receiving short-duration opioids intraoperatively.

Building a Simplified Remifentanil Target Controlled Infusion System

Authors: Elie Sarraf MD, CM; Donald M. Mathews MD

Introduction: The semi-synthetic opioid, Remifentanil, has been found to have versatile uses in the anesthetic practices that include induction for awake fiberoptic intubation [1] as well as the prevention of coughing during emergence [2]. While a target controlled infusion (TCI) system would simplify a quick titration to achieve a desired effect site concentration, this option does not presently exist in the United States. Consequently we demonstrate how to build a simplified bolus and infusion system, that can replicate a TCI pump from a zero initial state to a set final state, with simple arithmetic operations that can be performed with a basic spreadsheet. We then asses the performance of this system on several simulated patients.

Methods: The system design is conducted over a series of steps that are described in the appendix using the Minto Remifentanil model [3].

Using Matlab (R2016b) the above system was simulated with patients with the ages of 30, 50 and 70, weights between 50 and 110 kg in increments of 20 kg, heights of 120 and 210 cm in increments of 30 cm, as well as both genders. Patient with lean body mass (LBM) less than 20 kg were excluded from the analysis. The targeted concentration was 2.5 ng/mL. The normalized root-mean-squared error (NRMSE) was calculated to assess the system performance from 5 minutes to 30 minutes as a measure of the deviation from the target. This is calculated with the following formula:

$$NRMSE = \frac{\sqrt{\int_5^{30} \frac{(drug\_concentration(t) - target)^2}{30 - 5} dt}}{target}$$

Results: 96 simulated patients were simulated of which 9 had LBM < 20 kg and were excluded. Their effect site concentration over time is plotted in Figure 1. 4 patients are highlighted in Figure 1 and their characteristics are shown in Table 1. The mean NRMSE was 0.0423. The distribution of NRMSE is shown in Figure 2.

Conclusion: Using this technique one is able to quickly and effectively generate a bolus and infusion sequence that can mimic the performance of a simplified TCI system within a 7% error. This technique has been implemented on an online spreadsheet (http://bit.ly/2lXH0m8), but can equally be implemented in mobile apps as well as webpages. The clinical performance of the system has not yet been demonstrated.

References:

1. Lee HM, et al.. Korean J Anesthesiol. 2013: 65(3):215-20.

2. Lee B et al. BJA 2009: 102(6):775-8.

3. Minto CF et al. Anesthesiology 1997: 86(1):10-23.

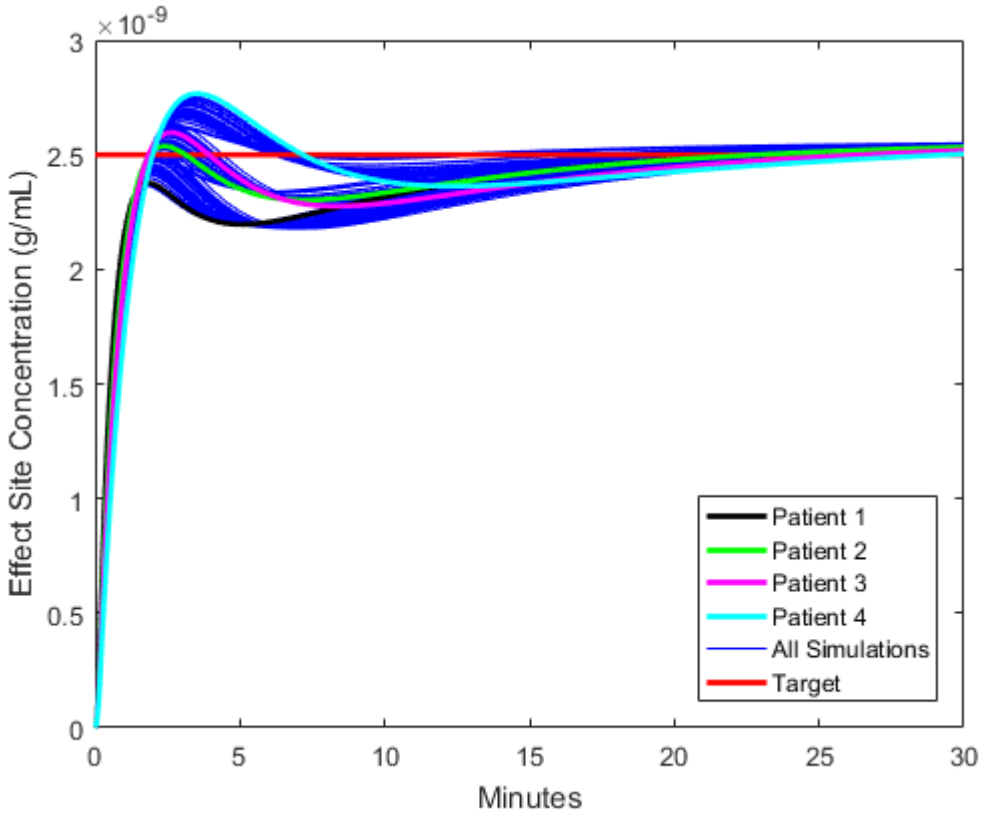

	Sex	Age	Weight (kg)	Height (cm)	Bolus (mcg)	Infusion (mcg/kg/min)	NRMSE
Patient 1	Female	30	50	120	25.6	0.117	0.052
Patient 2	Female	50	70	150	30.5	0.083	0.0411
Patient	Male	50	90	180	38.6	0.077	0.05

3							
Patient 4	Male	70	110	210	47.7	0.065	0.035

Figure 1: Effect site concentration over time plotted for 87 patient using method described in Appendix. 4 patients are highlighted in the figure whose characteristics are described in Table 1. Effect site goal is plotted as the thick red horizontal line

Table 1.Characteristic properties and bolus-infusion sequences of the four patients highlighted in Figure 1. The NRMSE is also calculated for those four cases

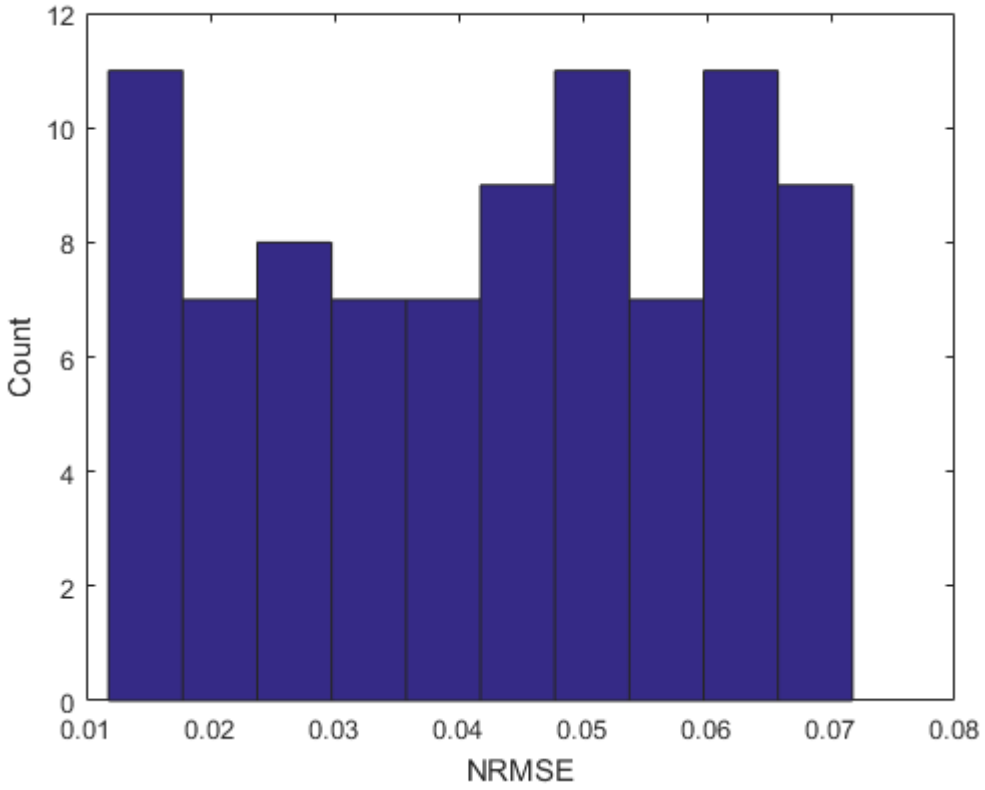

Figure 2: Distribution of the NRMSE for the performance of 87 simulated patients compared to a target.

Appendix:

1) Using the Minto model, calculate the patient's lean body mass, drug volumes, clearances and ke0.

2) Calculate the infusion rate by multiplying the desired effect site concentration by the metabolic clearance (Cl1). It is important to ensure proper unit conversions during this step

3) Calculate the bolus dose by multiplying the desired effect site concentration by the volume of distribution at peak effect. The latter can be determined by multiplying the primary compartment volume by the following ratio:

Ratio = 1.35 + 8.9/V1 - 0.669/Cl1 - 4.28/(V1*Cl1) – 0.154/Cl2 + 2.24/V2 - 1.22/LBM + 0.411/ke0

With LBM representing the lean body weight, V1 and V2, the volumes of the first and second compartments and Cl1, and Cl2, the clearance of the first and second compartments respectively. The derivation of this equation is described in another abstract.

4) Subtract from the bolus dose the amount of drug received during 1.5 minutes of the infusion

5) Multiply both the bolus and infusion rate by 1.045 to accelerate the pump's convergence to the desired target. This factor should be removed after 30 minutes.

Simplified Estimation of the Volume of Distribution at Peak Effect for Remifentanil

Authors: Elie Sarraf MD, CM; Donald M. Mathews MD

Pharmacokinetic mammillary models is described as a central compartment distributing a medications to peripheral compartments and is characterized by volumes of distributions of the compartments as well as their associated clearances. In addition, the volume of distribution at peak effect (V_{dpe}) [1], is a theoretical volume that relates the pharmacodynamics of the model after a bolus:

Loading dose = $C_{epe} * V_{dpe}$

Where C_{epe} is the plasma concentration of the drug at peak effect.

For a given patient, the ratio V_{dpe} to the volume of distribution of the central compartment (V_1) is constant and equal to the ratio between the initial plasma concentration (C_0) after a bolus to C_{epe}. This ratio can be determined through simulation by directly calculating C_0/C_{epe} or through non-trivial arithmetic computations.

We propose an alternative approach to determining the ratio through parameter estimation which we apply to Minto's remifentanil model [2]. This approach results in a simple method to calculate the ratio and thus V_{dpe}.

Methods: Using Matlab (R2016b), the C_{epe} along with the C_0 was determined for simulated patient between the ages of 20 and 80 in increments of 5 years, weights of 40 and 120 kg in increments of 5, heights of 120 and 220 cm in increments of 10 cm, as well as both genders. Patients with lean body mass (LBM) below 20 kg were excluded from further analysis. Age, weight, height, gender, LBM, volumes of distribution (V_1, V_2 and V_3), clearances (Cl_1, Cl_2, Cl_3), ke0 and the ratio C_0/C_{epe} were tabulated. Using R (version 3.3.2), a linear model was fit as a function of the ratio in an incremental fashion; the model performances were assessed using both Akaike information criterion (AIC) and Bayesian information criterion (BIC).

Results: 4862 patients were simulated of which 247 were excluded due to a low LBM. The distribution of the calculated ratio is shown in Figure 1. The ratio, as a function of V_1 is shown in Figure 2. Table 1 shows a series of fitted model as well as the calculated AIC and BIC. The optimal model is determined as:

$$\text{Ratio} = 1.35 + 8.9/V_1 - 0.669/Cl_1 - 4.28/(V_1*Cl_1) - 0.154/Cl_2 + 2.24/V_2 - 1.22/\text{LBM} + 0.411/\text{ke0}$$

Figure 3 shows the predicted ratio against the residual errors for the last model

Conclusion: By calculating the ratio with the above equation, one can effectively approximate the V_{dpe} with minimal computational power. The application of this estimate is demonstrated in an accompanying abstract. Whether this method can be extrapolated to other pharmacokinetic models has yet to be determined.

References

1. Flood P et al. Stoeting's Pharmacology & Physiology in Anesthetic Practice, 5th ed, Wolters Kluwer Health, p 31-32
2. Minto CF et al. Anesthesiology 1997: 86(1):10-23.
3. R Core Team (2014). R: A language and environment for statistical computing. R Foundation for Statistical Computing, Vienna, Austria. URL http://www.R-project.org/

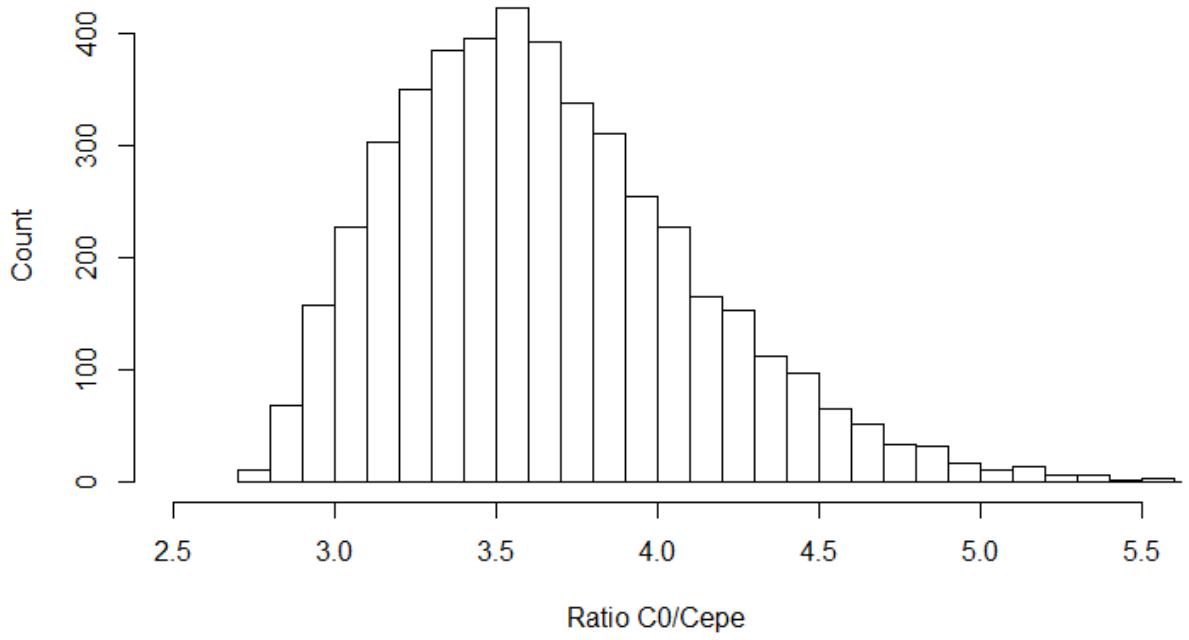

Figure 1: Distribution of the calculated ratio of the initial plasma concentration (C_0) to the plasma concentration of the drug at peak effect (C_{epe}) is shown for all simulated patients.

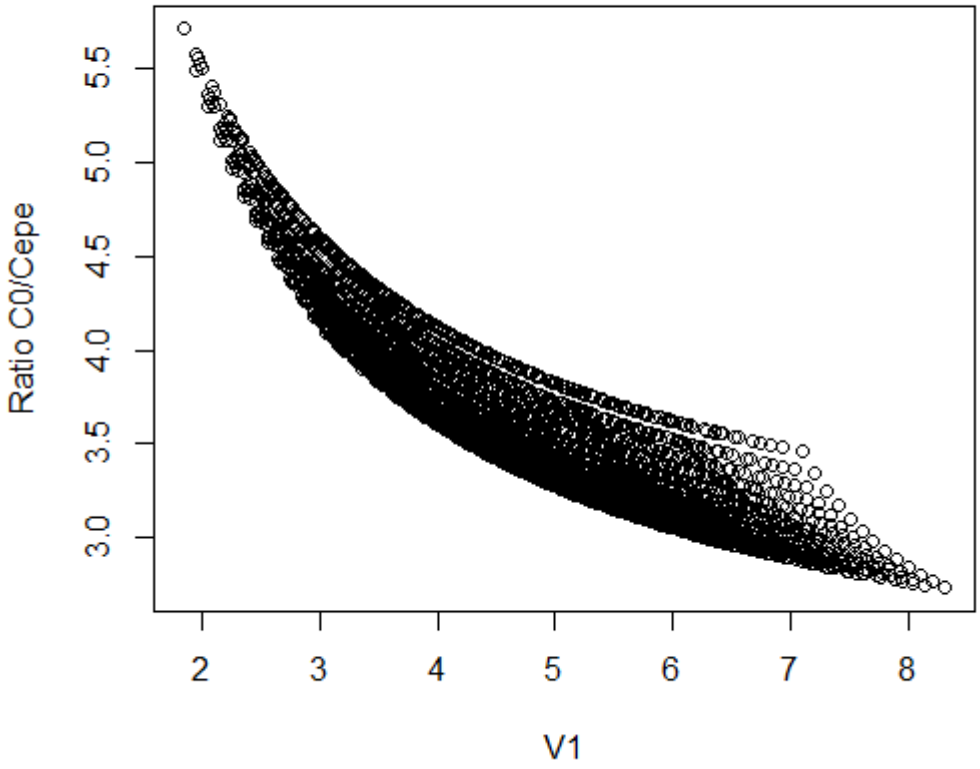

Figure 2: Calculated ratio as a function of V_1 for all simulated patients

		AIC	BIC
Model 1:	$1/Cl_1$	-9983.8	-9964.4
Model 2:	Model 1 + $1/V_1$	-15318	-15344
Model 3:	Model 2 + $1/(V1*Cl_1)$	-15453	-15421
Model 4:	Model 3 + $1/Cl_2$	-26943	-26905
Model 5:	Model 4 + $1/V_2$	-31313	-31268
Model 6:	Model 5 + 1/LBM	-53299	-53248
Model 7:	Model 6 + 1/ke0	-56001	-55943

Table 1: Performance of fitted models to estimate the calculated ratio as determined by AIC and BIC

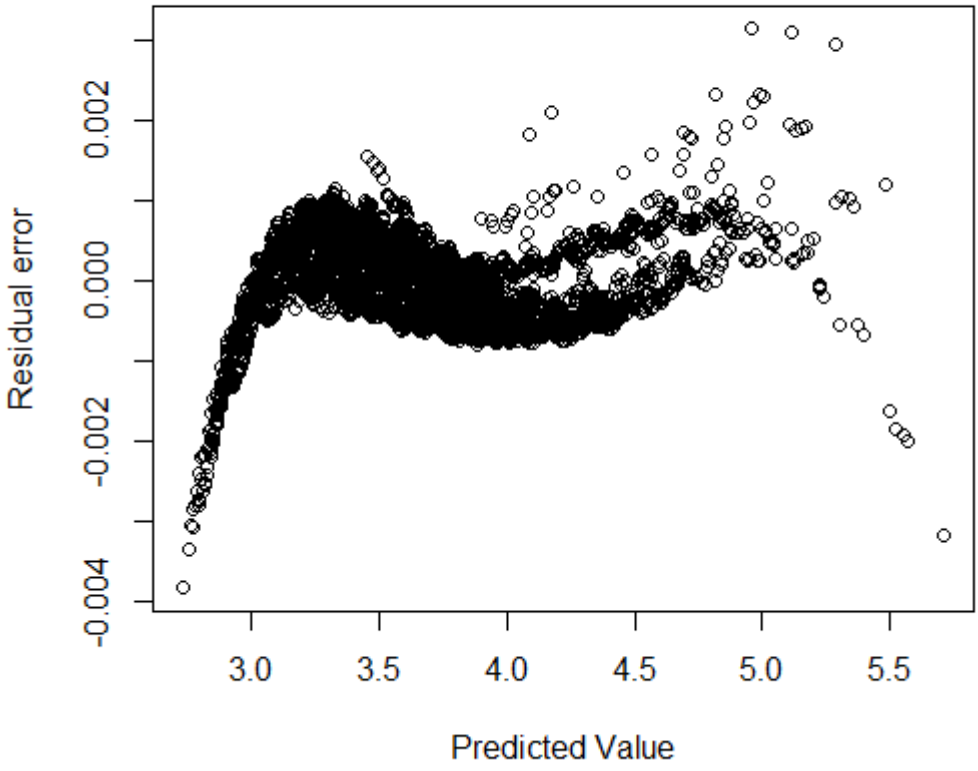

Figure 3: Scatter plot for the predicted ratio of the final model against each estimate's residual error

Comparing End-Tidal and Calculated Effect-Site Sevoflurane Concentrations at Awakening from Anesthesia

Presenting Author: Ross Kennedy [1,2]
Co-Authors: Margie McKellow [1], Jonathan Williman [3]

[1] Department of Anaesthesia, Christchurch Hospital, Christchurch NEW ZEALAND
[2] Department of Anaesthesia, University of Otago - Christchurch, Christchurch NEW ZEALAND
[3] Department of Population Health, University of Otago - Christchurch, Christchurch, NEW ZEALAND

Background/Introduction: The relationship between drug dosing and effect is complex. This is especially so of many drugs used in anesthesia where the effect may need to be changed well before equilibrium is reached. It has been suggested that using calculated effect-site concentrations (Ce) can improve titration of intravenous anesthetic drugs. We are interested in the proposition that effect-site concentrations of volatile anesthetic agents can provide useful information for the provider especially during periods of rapid change when the delay between measured end-tidal and effect-site concentration will be greatest.

We have previously demonstrated that subjects wake, on average, at Ce-sevoflurane close to MAC-awake. This observation supports the concept of Ce for volatiles, since MAC values are assumed to represent equilibrium.

The aim of the this study is to compare calculated Ce and measured end-tidal (ET) sevoflurane concentrations at awakening in a wide range of patients and procedures.

Methods: With National Ethics Board approval, data was collected from ASA 1 -3 patients undergoing procedures where the anesthetic plan was based on sevoflurane and fentanyl. This is an opportunistic sample, dependant on the availability of the research assistant and GE_Navigator. The only change to normal practice was to keep patients attached to the anesthesia machine and monitors until awakening with a minute ventilation ≥ 3l/min ≥ 5 breaths/min to ensure monitored end-tidal concentrations represented alveolar, rather than breathing circuit, gas. Awakening time was when the patient first responded to spoken command (OAA/S =4/5, similar to MAC-awake studies). Effect-site concentrations were taken from the Navigator data files. ET and Ce concentrations were adjusted for age.

Results: We have paired data from 74 subjects. Age range 18-86, median 52; BMI median 27, [IQR 24-32] kg/m^2. Duration of anaesthesia median 94 [75-149] min. Median age adjusted Ce-sevo was 0.51 [0.40-0.66] vol% while age-adjusted ET sevo concentration was 0.29 [0.24-0.35] vol%. The median difference between Ce and ET was 0.25 [0.15 to 0.35] vol%. Median fentanyl Ce at response was 2.2 [1.8-2.9]ng/ml

There was a weak correlation (p=0.0017) between age-adjusted Ce and ET values; (95%CI of slope 0.05 to 0.26). There was no correlation between age or duration of surgery with either Ce or ET values.

Conclusions: We have confirmed our previous observation that pooled, age-adjusted Ce-sevoflurane concentrations at wake-up are similar to MAC-awake amd demonstrated that end-tidal values at this time are much lower. While this result would be expected by those familiar with effect-site concepts, it is often considered that end-tidal values are “close enough”. Our data suggests that this may not be the case during rapid changes and may be useful in discussions about the role of Ce.

Combined Recirculatory-Compartmental Population Pharmacokinetic Modeling of Arterial and Venous S(+) and R(-) Ketamine Concentration Data

Presenting Author: Thomas K. Henthorn[1]
Co-Authors: Erik Olofsen[2], Michael J. Avram[3], Tom C. Krejcie[3], Jan Persson[4], Lars L. Gustaffson[4], Albert Dahan[2]

[1]Anesthesiology, Univ of Colorado, Aurora, CO [2]Anesthesiology, Leiden Univ Med Center, Leiden, NL; [3]Anesthesiology, Northwestern Univ, Chicago, IL; [4]Clinical Pharm, Karolinska Inst, Huddinge, SE

Introduction/Background: To date, pharmacokinetics (PK) of ketamine and other drugs infused by a constant rate infusion have been modeled without regard for recirculatory or mixing kinetics. We used a unique, ketamine dataset with simultaneous arterial and venous sampling, obtained during and after separate S(+) and R(-) ketamine infusions to develop a simplified recirculatory model of arterial and venous drug concentrations. We postulated that with A-V data, cardiac output and, thus, recirulatory kinetics could be directly estimated.

Methods: 7 mg of S(+) and R(-) ketamine were infused over 30 minutes on two occasions to 10 healthy male volunteers. Frequent, simultaneous arterial and forearm venous blood samples were obtained during and for up to 11 hours after the start of infusion. A multi-compartmental pharmacokinetic model with frontend mixing (cardiac output) and forearm kinetics, using a technique similar to an effect compartment model (see figure), was developed using population non-linear mixed effects analyses.

Results: A 3-compartment PK model with arterial mixing and arm venous compartments and with shared S(+)/R(-) distribution kinetics proved superior to standard independent compartmental modeling approaches. Cardiac output was estimated to be 6.52 $\pm$ 0.67 l/min (median $\pm$ SE) and S(+) and R(-) clearance were 1.33 $\pm$ 0.06 and 1.11 $\pm$ 0.05 l/min, respectively. The fraction of arm blood flow estimated to exchange with arm tissue was 0.05 $\pm$ 0.01; K_{arm0} (analogous to K_{e0}) was 0.11 $\pm$ 0.06 min^{-1} and tissue:plasma partition ratio was 3.90 $\pm$ 98.
Discussion: The current study shows that arterial drug concentrations measured during drug infusion have an 'infusion artifact' due to unmixed drug. Recirculatory kinetics demonstrate that this concentration artifact is equal to the ratio of infusion rate and cardiac output. This simplified frontend modeling approach could lead to more generalizable models for TCI and improved methods for analyzing PKPD data.
Figure 1.

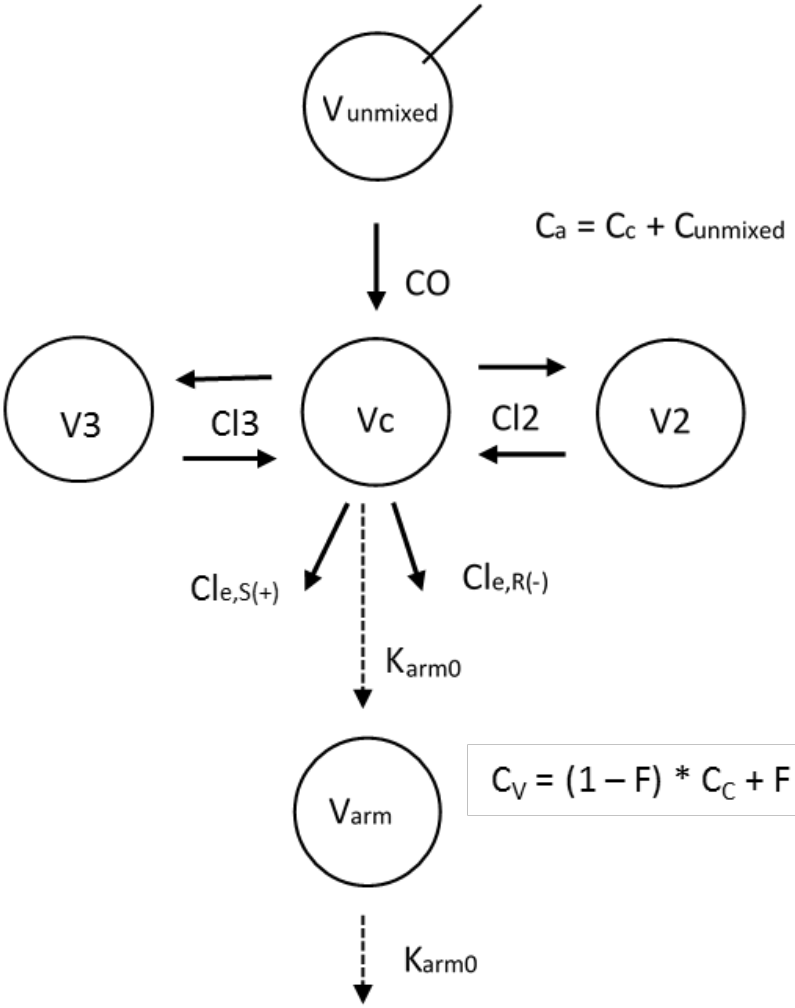
Vunmixed
Ca = Cc + Cunmixed
CO
V3
Cl3
Vc
Cl2
V2
Cle,S(+)
Cle,R(-)
Karm0
Varm
CV = (1 – F) * CC + F * Carm * PCarm
Karm0

Norbuprenorphine Pharmacokinetics and Pharmacodynamics: First in Man Evaluation

Presenting Author: Evan D. Kharasch[1,3]

Co-Authors: Thomas K. Henthorn,[2] Alicia M. Flaker,[1] Kristi Kraus,[1] Jane Blood[1]

[1]Department of Anesthesiology, Washington University in St. Louis, St. Louis, MO;
[2]Department of Anesthesiology, University of Colorado School of Medicine, Aurora, CO,
[3]The Center for Clinical Pharmacology, St. Louis College of Pharmacy and Washington University School of Medicine St. Louis, MO

Background: Buprenorphine (Bup) is a partial μ agonist, δ and κ antagonist, and nociceptin receptor agonist, with complex pharmacology. It is extensively metabolized, primarily to norbuprenorphine (norBup); both Bup and norBup undergo glucuronidation. Metabolite exposure can exceed that of Bup. NorBup, Bup-glucuronide and norBup-glucuronide are pharmacologically active. Mechanisms of Bup pharmacology in humans remain undefined. This investigation evaluated norBup clinical pharmacology, including PK, clinical effects and PD, in two first in man, IRB-approved, single-center protocols in healthy volunteers.

Methods: Protocol 1 was an open label dose-escalation (0.005-1 mg, 1 hr infusion) pilot, to evaluate dose-dependent PK and clinical effects of NorBup. Venous plasma was sampled for up to 13 hr, and urine collected for 24hr. Protocol 2 subjects received a fixed-dose 0.3 mg 1-hr infusion of NorBup. Arterial (radial) and venous plasma was sampled for 13 hr and 96 hr, respectively. Pupil diameter, respiratory rate, end-expired CO_2, and subjective self-assessment of drug effect were recorded. Response to thermal stimulus (Peltier thermode analgesia), was assessed using the methods of limits (maximal tolerated temperature) and ramp and hold method (VAS pain rating to a predetermined temperature). NorBup and NorBup-glucuronide were quantified by LCMS. Population PK modeling was performed with Phoenix 64 NMLE 7.0 using the FOCE ELS algorithm (Certara). Model parameters were assumed to be log-normally distributed across the population. Independent PK models for arterial (NorBup & NorBup-glucuronide) and venous (NorBup & NorBup-glucuronide) were tested against a minimal, comprehensive model that linked arterial and venous drug/metabolite concentrations, using recirculatory model principles, and a metabolic tanks-in-series pathway. Criteria for accepting the linked model were improvement of -2LL of at least 3.84 and reduction in AIC (Chi squared, $p<0.05$). Urine drug and metabolite concentrations were incorporated in the respective models as cumulative drug or metabolite collected at each collection time point.

Results: NorBup was well-tolerated, without adverse effects. Plasma norBup-glucuronide exceeded norBup concentrations. NorBup and norBup-glucuronide plasma AUCs, and urine excretion, were proportional to dose ($r>0.9$) throughout the entire dose range. NorBup-glucuronide was formation-rate limited. NorBup arterial concentrations were 2x venous concentrations during the infusion, and similar thereafter with venous

systematically higher. The A-V difference was well modeled with a linked 3-compartment base model and a recirculatory mixing component with a typical cardiac output of 6.5 L/min. NorBup to the glucuronide tvCl was 342 ml/min and renal tvCl of NorBup-glucuronide was 125 ml/min, based on urine collection. Non-renal clearance accounted for 91% of NorBup and 71% of NorBup-glucuronide clearances. NorBup (0.3 mg) caused mild miosis (maximum pupil diameter change 1.3 ± 0.8 mm), minimal respiratory depression (respiratory rate decreased from 16 ± 1 to 14 ± 3 and end-expired CO_2 increased from 39 ± 2 to 41 ± 2 mmHg), and was slightly anti-analgesic (maximum tolerated temperature decreased from 49 ± 1 to 48 ± 1 °C and NRS pain ratings to a preset temperature increased to 113 ± 13% of baseline). Effect (miosis) vs concentration showed hysteresis.

Conclusions: NorBup is pharmacologically active in man, shows both μ agonist and κ antagonist properties and may contribute to the pharmacologic effects of parent Bup.

Generation of EEG Oscillations in Isolated Neocortical Brain Slices

Authors: Noelie S.J. Cayla, and M. Bruce MacIver
Department of Anesthesiology, Perioperative and Pain Medicine, Stanford University School of Medicine

Introduction: Different frequencies of oscillatory neuronal activity can be produced in rodent neocortical slices by pharmacologically mimicking cholinergic inputs to the cortex during attention and increased glutamatergic excitation during active behaviors. The present study looked at neocortical oscillations produced by application of combined neurotransmitters in rat brain slices.

Methods: 400 µm-thick brain slices were prepared from 24-28 days old Sprague-Dawley rats, and they were incubated for two hours at 32°C with oxygenated Artificial Cerebrospinal Fluid (ACSF). Extracellular neuronal population activity (micro-EEG) was recorded with glass microelectrodes from layer 2/3 of neocortex (Oc2MM in the Retrosplenial cortex). We stimulated cortical neurons in two ways: electrically by driving and thalamic and cortical inputs or chemically by adding combinations of drugs that activate glutamatergic, histamine or cholinergic pathways. Data were collected, analyzed and stored using Igor Pro software (Wavemetrics, OR).

Results: We found that *in vivo*-like EEG oscillations are produced in slices with application of drugs influencing glutamatergic and cholinergic or histaminergic receptors. Most past work has shown that the production of oscillations is dependent on two factors: excitation of neuronal populations and a level of disinhibition. In this study, we show that application of carbachol (cholinergic agonist) and bicuculline (competitive antagonist of $GABA_AR$) effectively produced EEG oscillations. We also show that theta oscillations can be produced without disinhibition, using carbachol and by activating glutamatergic inputs through the addition of kainate. We show that muscarinic and not nicotinic receptors are more important in the production of these oscillations. Lowering the magnesium concentration from control conditions (2 mM) to 0.5 mM allowed NMDA gated glutamate receptors to also come into play and this produced even more robust oscillations. Moreover, the importance of glutamatergic stimulation was observed with the reversible block of oscillations by 2-amino-5-phosphonovaleric acid (APV, 100 μM), an NMDA receptor antagonist.

Conclusions: We report for the first time that theta oscillations can occur without disturbing GABA-mediated inhibition by co-activating kainate receptors. Our ultimate goal is to mimic *in vivo* EEG oscillatory behavior in brain slices. This would facilitate the mechanistic studies of normal cognitive signal processing circuitry and also how anesthetics alter this circuitry.

Remifentanil and Nitrous Oxide Anesthesia Produces a Unique Pattern of Frontal EEG Activity

Presenting Author: Sarah Eagleman[1] PhD

Co-Authors: David R Drover[1] MSc MD, Caitlin Drover, and M Bruce MacIver[1] MSc PhD

[1]Anesthesiology, Perioperative and Pain Medicine, Stanford University School of Medicine

Introduction: Remifentanil (remi) and nitrous oxide (N_2O) are commonly used in combination, together with other anesthetics, for routine surgical anesthesia, yet the electroencephalogram (EEG) effects of these are poorly described. In addition, remi and N_2O produce EEG effects that are difficult to analyze using traditional frequency-derived measures. The present study examined effects of these two agents on EEG signals recorded from 40 randomly chosen surgical patients.

Methods: EEG responses were recorded using a BIS monitor, following patient consent to a Stanford University approved protocol. Remifentanil concentrations were varied on a steady background of nitrous oxide (66%) and cortical responses to a train of four (TOF) stimulus were compared at different concentrations of remi.

Results: At surgical planes of anesthesia high amplitude slow waves (1 to 2 Hz) dominated the EEG, similar to effects seen with most anesthetics, but these slow waves were interspersed with rhythmic theta activity from 4 to 10 Hz that lasted a few seconds to several minutes before reverting to slow wave activity, that could also last several seconds to minutes. Changes in remi concentrations had little effect on background activity, marginally increasing slow waves, and did not change the alternating pattern of delta and theta activity. Chaos analysis of the same EEG signals showed a typical flatting of attractors that is seen with propofol as well as with volatile anesthetics. Attractor flattening was seen for both the delta and theta dominant EEG patterns, with little apparent difference, at surgical planes of nitrous oxide/remifentanil anesthesia. TOF stimulation produced cortical activation, seen as a marked decrease in signal amplitude and increase in higher frequency content, which was diminished by higher concentrations of remi.

Conclusions: We conclude that remi/N_2O anesthesia is associated with a unique oscillating pattern of delta/theta frequency activity that makes it difficult to correlate these frequency-derived measures with anesthetic depth. Chaos analysis, in contrast, consistently provided a good measure of anesthetic depth in these patients.

Supported by: NIH GM095653 and Stanford Anesthesia

BDNF Gene Polymorphisms and Chronic Postsurgical Pain

Authors: Matthew Chan, Yuanyuan Tian, Xiaodong Liu, William Wu, Tony Gin
Department of Anaesthesia & Intensive Care, The Chinese University of Hong Kong, Hong Kong SAR

Background: Chronic postsurgical pain affects at least 10% of patients undergoing common operations and adversely affects their quality of life. We evaluated the genetic association between single-nucleotide polymorphisms (SNPs) and chronic postsurgical pain.

Methods: Using GoldenGate genotyping assays, we genotyped 768 SNPs within 65 pain-related genes in 1,152 surgical patients who were enrolled in our Persistent Pain After Surgery Study. Patients were contacted by phone to determine if they had chronic postsurgical pain at 12 months. SNPs identified were validated in a matched cohort of 103 patients with chronic postsurgical pain and another 103 patients who were pain-free. Functional role of the targeted SNP was tested in an experimental plantar incision pain model using knock-in mice.

Results: At 12 months after surgery, 246 (21.4%) patients reported chronic postsurgical pain. SNPs located in brain-derived neurotrophic factor (*BDNF*) gene (*rs6265* and *rs1491850*) were significantly associated with chronic postsurgical pain, p=0.003 and 0.004, respectively. The effects of both SNPs were confirmed in the validation cohort, p=0.005 and 0.002, respectively. Age <65 years, male gender, low education level and prior history of pain syndrome were found to increase risk of chronic postsurgical pain. The two SNPs had higher population attributable risk (6.25-12.3%) compared with clinical risk factors (3.71-8.76%). Importantly, the functional role of *rs6265*, which is a non-synonymous SNP, was confirmed with less mechanical allodynia in $BDNF^{Met/Met}$ mice compared with $BDNF^{Val/Val}$ group after plantar incision (Figure 1).
Conclusions: This study demonstrated that genetic variations of *BDNF* is important in determining the susceptibility to chronic postsurgical pain.

Figure 1. Incisional pain mouse model. A 10-mm longitudinal incision was made on the plantar surface of the left hind paw. Changes in paw withdrawal in response to pressure using von Frey filaments in $BDNF^{Met}$ knock-in (Met/Met) and wild-type (Val/Val) mice (n = 15 per group). *, $p < 0.05$, repeated measures analysis of variance; Values are mean ± standard error.

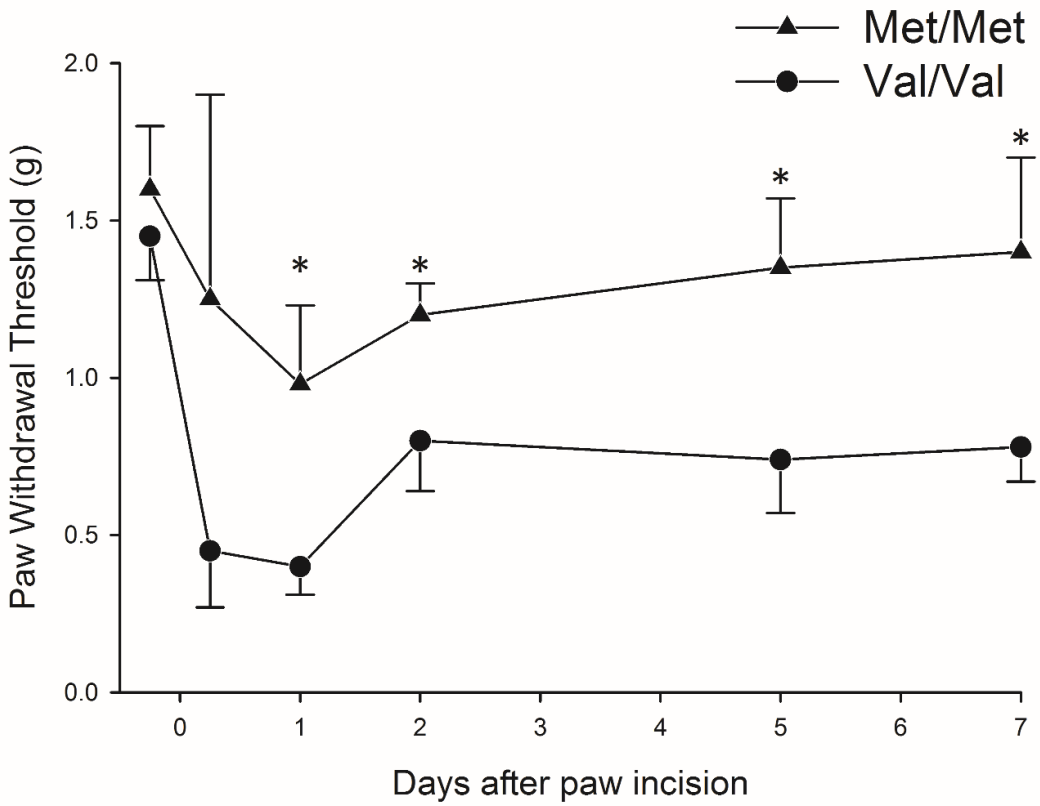
Met/Met
Val/Val
Paw Withdrawal Threshold (g)
2.0
1.5
1.0
0.5
0.0
0
1
2
3
4
5
6
7
Days after paw incision
*
*
*
*

Brief Pediatric Cases Use a Similar Mass of Sevoflurane as Adult Anesthetics Lasting Over an Hour

Presenting Author Ross Kennedy [1,2]
Co-authors Ben van der Grind[1], John Page[3], Guy Vesto[3] , Richard French[1]
[1] Department of Anaesthesia, Christchurch Hospital, Christchurch NEW ZEALAND
[2] Department of Anaesthesia, University of Otago - Christchurch, Christchurch NEW ZEALAND
[3] GE Healthcare, Madison WI

Background / Introduction: It is established that volatile anaesthetic agents come with an economic and environmental cost. Over recent years, considerable gains have been made to reduce fresh gas flow (FGF) and thus agent waste during volatile anaesthesia. However, in paediatric anaesthesia, high FGFs are still commonly employed especially during induction, but also during maintenance of anaesthesia.

Methods: Data for this study was collected as part of an ongoing collaboration between CDHB and GE-Healthcare looking at data routinely logged during anesthesia, with an emphasis on fresh gas flow rates.

We compared sevoflurane usage from 200 anaesthetic episodes of 20 minutes or less duration for myringotomies with ventilation tubes or adenoidectomies in pediatric patients with that of 536 anesthetics where sevoflurane was used for adult general surgery in a single OR.

Results: For the pediatric cases, the median duration was 13 minutes and the duration of agent delivery as 8 minutes [IQR 6-10]. The median amount of sevoflurane used was 13 mL [IQR 10-15]. For cases performed with a circle system, 12 ml of sevoflurane was used. With a T-piece (open system), 14 ml of liquid sevoflurane was used.

In comparison, the median duration of adult general surgery cases was 86 minutes and the duration of agent delivery was 68 minutes [IQR 38-120]. The median amount of sevoflurane used was 12 mL [IQR 8-17].

Conclusions: A median of 8 minutes of agent delivery for pediatric anaesthesia (for ventilation tubes or adenoidectomies) consumed a similar amount (slightly more) sevoflurane than 68 minutes (over 8 times) of agent delivery for adult anaesthesia.

While there are significant differences in the anesthesia practice and requirements in these groups (eg intravenous *vs* inhalational induction) these results highlight the inefficient use of sevoflurane common in paediatric anaesthetic practice.

Gas Flow in the Induction Period Can Have a Significant Effect On Overall Gas and Vapour Consumption Despite Low Maintenance Flows

Presenting Author Ross Kennedy [1,2]
Co-authors Richard French[1], James Hanrahan[3], Guy Vesto[3]
[1] Department of Anaesthesia, Christchurch Hospital, Christchurch NEW ZEALAND
[2] Department of Anaesthesia, University of Otago - Christchurch, Christchurch NEW ZEALAND
[3] GE Healthcare, Madison WI

Background / Introduction: RK and RF have a long interest in reducing FGF to reduce cost and environmental impact and are collaborating with GE-Healthcare exploring data from anaesthesia delivery systems.

The duration of, and FGF during the “high flow” phase have a marked effect on overall mean FGF as illustrated by our “two-box” model and simple mathematical modelling which shows that for a 90 min case with a maintenance FGF 2l/min and initial FGF 6l/min, reducing the high flow period from 10 to 2 min reduces mean FGF from 2.44l/min to 2.09l/min, or 14%. This early phase is not included in several studies of FGF.

Here we present our models and updated FGF data from >4000 cases demonstrating the influence of a simple intervention directed at encouraging anesthesiologists to avoid extreme FGF and minimise the duration of the initial high flow period.

Methods: Data is logged from 4 GE-Aisys CS2 Carestations equipped with end-tidal control, in OR with a diverse mix of practice and providers. Data is analysed using rules to divide the time vapour is being delivered into blocks. The high flow period begins at the start of the case and ends once FGF drops below 5l/min.

Over 2 weeks we provided all anesthesiologists with repeated information on the importance of FGF in this high-flow phase. We compared the pattern of flow rates in (A) 3 months before this intervention, (B) 2 months immediately following and (C) the 5 months following period B. Mean FGF is a marker of vapour consumption. Kruskal-Wallis test used for comparisons.

Results: We now have data on 3190 vapour based anesthetics from 4 rooms. Pooled results are shown in the table as median [IQR]. The changes in duration and FGF during high flow phase are significantly different from A. Overall FGF decreased from A -> B but increased slightly in period C (A & C not significantly different) driven predominantly by a small rise in maintenance FGF.

	N	Initial FGF (l/min)	Duration of initial hi flow (min)	Maintenance FGF (l/min)	Time weighted mean FGF (l/min)
A	1389	6 [6, 6]	2 [0, 4]	0.5 [0.5, 0.60]	0.823
B	500	6 [0, 6]	1 [0, 3]	0.5 [0.5, 0.55]	0.736

C	1301	6 [0, 6]	2 [0, 4]	0.5 [0.5, 0.66]	0.809

Conclusions: Most efforts to reduce FGF focus on the maintenance phase. We have shown that the duration and gas flows during the early phase can have a profound effect on gas and vapor use. This effect is also seen with moderately high maintenance flows.

We observed the FGF used for pre-oxygenation was frequently maintained after induction. Although our average flows are already very low, we were able to produce an additional 10% reduction and can identify opportunities for further improvement.

Cerebral Blood Flow Changes Assessed by System Complexity Measures Applied To Cerebral Bioimpedance Signals

Authors: C.González[1,2], E.W. Jensen[2], P.L. Gambús[3], M.Vallverdú[1]

[1] Biomedical Engineering Research Centre, Universitat Politècnica de Catalunya, CIBER of Bioengineering, Biomaterials and Nanomedicine (CIBER-BBN), Barcelona, Spain

[2] Quantium Medical, Research and Development Department, Mataró, Spain

[3] Hospital Clínic de Barcelona, Dept of Anaesthesiology, Barcelona, Spain

Background/Introduction: Monitoring cerebral blood flow during anesthesia is of great interest, mainly during surgeries with an associated risk of stroke. A non-invasive, real time and cost-effective method for that purpose could be based on cerebral impedance measurements. As apnea alters cerebral blood flow [1], a comparison between apnea and baseline cerebral impedance waves (CIW) processed by means of Poincaré plots is presented a proof of concept of this proposal.

Methods: Data from 16 healthy subjects were recorded during both resting periods (baseline) and apneas, in supine position, repeating twice the sequence resting period – apnea. Baseline recordings lasted 3 minutes while apneas 1 minute, unless they were interrupted earlier by the volunteer. System-complexity measures were extracted from those signals by means of building the Poincaré plot of the corresponding attractors, defined as a state space representation of the behavior of a complex system. Attractors were built for every 16 seconds of signal and two main features were extracted: the ratio between the standard deviations on the identity line and its perpendicular line (SD ratio) [2] as shown in figure 1, and the correlation of the Poincaré map (R) as defined in [3]. The Mann-Whitney U-test was used to test for significant differences ($p<0.05$) between CIW at baseline and apnea.

Results: Participants were healthy volunteers aged 25.4 ±3.6 years, 59.6 ± 6.8 kg weight and 166.9 ±8.3 cm height. After data collection, periods affected by artefacts caused by movements, eye blinking or swallowing were excluded from the analysis. 53 sequences were extracted from the 16 volunteer recordings, 29 from apneas and 24 from baseline periods. SD ratio and R were computed for attractors built from the recorded signals (figure 1), resulting in statistically significant differences for both parameters at different attractor time lags (table1). No statistically significant differences were detected for heart rate in both groups.

Conclusions: The proposed method allows characterization of cerebral impedance waves in order to distinguish between baseline recordings and apnea episodes, in which cerebral blood flow is known to be altered, even when no differences in heart rate are detected. SD ratio and R measurements on attractors might be a powerful tool for fast brain perfusion assessment during anesthesia.

References

[1] Kastrup, A., Krüger, G., Neumann-Haefelin, T., & Moseley, M. E. (2001). Assessment of cerebrovascular reactivity with functional magnetic resonance imaging: comparison of CO 2 and breath holding. Magnetic resonance imaging, 19(1), 13-20.

[2] K. Hayashi, N. Mukai, and T. Sawa, “Poincaré analysis of the electroencephalogram during sevoflurane anesthesia,” Clin. Neurophysiol., vol. 126, no. 2, pp. 404–411, 2015.

[3] M. Brennan, M. Palaniswami, and P. Kamen, “Do existing measures of Poincare plot geometry reflect nonlinear features of heart rate variability?”, IEEE Trans. Biomed. Eng., vol. 48, no. 11, pp. 1342–1347, 2001.

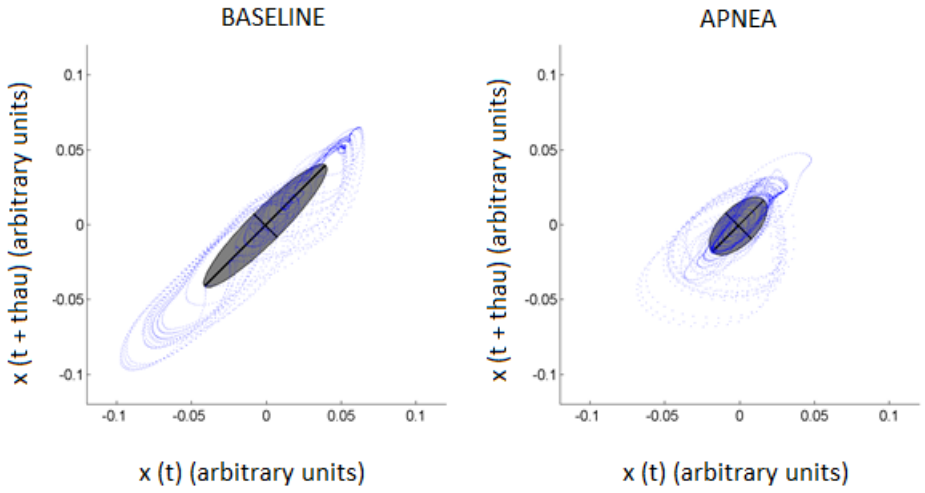

Figure 1: Poincaré plot of a CIW, with time lag thau = 5, from a baseline period (left) and apnea (right) illustrating the SD1 and SD2 features as the axis of the ellipse.

Table 1: mean (SD) values (arbitrary units) obtained for each parameter and the corresponding time lag (signals were sampled at 250 samples per second)

Time lag (samples)	SD ratio		R		p-value
	Baseline	Apnea	Baseline	Apnea	
5	0.114 (0.027)	0.142 (0.032)	0.973 (0.014)	0.959 (0.020)	
10	0.221 (0.054)	0.277 (0.066)	0.903 (0.049)	0.853 (0.069)	
15	0.320 (0.081)	0.401 (0.103)	0.809 (0.092)	0.719 (0.126)	
20	0.407 (0.107)	0.510 (0.140)	0.711 (0.132)	0.587 (0.172)	$p < 0.001$
25	0.485 (0.131)	0.603 (0.170)	0.617 (0.164)	0.473 (0.196)	
30	0.556 (0.150)	0.679 (0.183)	0.529 (0.185)	0.380 (0.199)	
35	0.623 (0.165)	0.742 (0.174)	0.446 (0.199)	0.302 (0.185)	
40	0.688 (0.176)	0.795 (0.151)	0.367 (0.207)	0.234 (0.163)	$p < 0.01$
45	0.753 (0.184)	0.846 (0.126)	0.289 (0.212)	0.173 (0.139)	

Anesthesia Sensitivity in $GABA_A$ β3 Subunit Mutant Zebrafish

Presenting Author: Xiaoxuan Yang
Co-Authors: Xiaoxuan Yang,[1,2] Youssef Jounaidi,[1] Eric C. Liao,[3] Stuart A. Forman[1]
[1]Department of Anesthesia Critical Care & Pain Medicine, Massachusetts General Hospital, Boston, MA, USA;
[2] Department of Anesthesiology, Ruijin Hospital, Shanghai Jiaotong University School of Medicine, Shanghai, China;
[3]Center for Regenerative Medicine, Massachusetts General Hospital, Boston, MA, USA

Introduction: The anesthetic action target γ-aminobutyric acid type A receptor ($GABA_AR$) exhibits diverse subunit heterogeneity. Based on studies in transgenic mice, the β3 subunit of $GABA_AR$ mediates anesthetic effect of etomidate, propofol, and pentobarbital. We have applied the zebrafish model to characterize general anesthetic potencies and drug discovery. In this study, we generated global $GABA_AR$-β3 mutants using CRISPR-Cas9 and compared their sensitivity to various general anesthetics with that of wild-type (WT) zebrafish.

Methods: CRISPR-Cas9 gene targeting and embryonic stem cell technologies were used to create β3-/- zebrafish. Guide RNA targeting on exon 7 of β3 subunit was injected into one-cell stage embryos. Anesthetic potency of etomidate, propofol, alphaxalone, ketamine, pentobarbital, tricaine, ethanol and butanol were determined using photomotor response in 7-day post fertilization larvae. Sedative effects were also measured with pre-flash spontaneous activity. 16~24 larvae/ concentration were included for each assay. Individual larvae movements were tracked using a video system (ViewPoint Zebralab), which also coordinated stimuli. Non-linear least squares fits to logistic equations were used to derive EC_{50} from potency test. Extra sum-of-squares F test was used to determine whether EC_{50} from β3-/- and WT were statistically different.

Results: Genome analysis revealed a 10bp insertion in exon 7 of $GABA_AR$-β3, introducing a premature stop-codon on mRNA and thereby truncation of protein from extracellular domain of the receptor. $GABA_AR$-β3 mutants did not differ in embryogenesis and fertility from WT, but were significantly more resistant to anesthetic effect of etomidate, propofol, pentobarbital, butanol and more sensitive to ethanol. No differences in anesthetic effect were noted in ketamine and tricaine (See Table 1). Similar changes in sedative effects were also observed except for ketamine where β3 -/- were more resistant to ketamine (β3 -/- [EC_{50}] of 0.1μM *vs.* WT [EC_{50}] of 0.04μM, $P<0.0001$).

Conclusions: Our findings demonstrate the anesthetic sensitivity phenotype of GABR-β3 mutant zebrafish, supporting the utility of this model to investigate mechanism of novel anesthetics acting through $GABA_AR$-β3 and normal neuro-physiology process.

Table 1: Comparison of anesthetics potency between β3 -/- and WT

Anesthetics	**β3 -/- [EC_{50}]**	**WT [EC_{50}]**	***P* value**
etomidate	1.12μM	0.55 μM	0.0001
propofol	1.03μM	0.72 μM	0.0029
pentobarbital	229.5μM	103.4 μM	0.0001
butanol	7.8mM	1.9mM	0.0001
ethanol	235.0mM	375.6mM	0.0013
alphaxalone	1.15μM	1.23μM	0.83
ketamine	55.7μM	50.6μM	0.59
tricaine	99.5μM	76.9μM	0.1166

Volatile Anesthesia or TIVA? Any Differences for Changes in Cerebral Oxygen Saturation in Steep Trendelenburg Position with Pneumoperitoneum or Beach- Chair Position

Presenting Author: Tomoko Fukada
Co-Authors: Yuri Tsuchiya, Akiko Zaitsu, Hiroko Iwakiri, Makoto Ozaki, Minoru Nomura

Introduction: The robotic-assisted laparoscopic prostatectomy (RALP) needs patients be placed in steep Trendelenburg position with pneumoperitoneum (TP position). On the other hand, the beach-chair position (BC position) during arthroscopic shoulder surgery (SS) requires the sitting position (extreme head up). We hypothesized that cerebral oxygen saturation measured using near infrared spectroscopy (rSO_2 by INVOS 5100C) increases in TP position and decreases in BC position and evaluated differences seen with volatile anesthesia or TIVA technique.

Patients and Methods: After obtaining IRB approval and written informed consents, we recruited patients who underwent RALP or SS. Exclusion criterion was a history of cerebrovascular disease. During surgery, general anesthesia was maintained at bispectral index of 40–60 with desflurane (volatile anesthesia) or TIVA. Ventilation was maintained with 45% oxygen and air to obtain an end-tidal carbon dioxide tension of around 35–40 mmHg. Systolic blood pressure, measured by a transducer at the cardiac level, was maintained around 130 mmHg. Before anesthesia induction, rSO_2 sensors were applied to the right and left forehead and lower legs.

Results: We so far, evaluated 26 of RALP and 15 of SS patients and found that rSO_2 did not change in TP position but decreased in BC position (Figure 1). There were NO differences in changes in rSO_2 between the anesthesia techniques, volatile anesthesia or TIVA. In addition, there were no significant neurogenic complications in any of the patients, even in those with low rSO_2 during surgery in BC position.

Discussion and Conclusion:
Interpretation of rSO_2 changes during general anesthesia in RALP or SS remains controversial. Because what percentage of reduction of rSO_2 would be

clinically significant is depends on multiple factors including individual patient characteristics and stress of surgery. Nonetheless, we confirmed in this small study that the TP position could be no significant influence for the cerebral oxygenation but the BC position would decrease it regardless of the anesthesia technique, volatile anesthesia or TIVA.

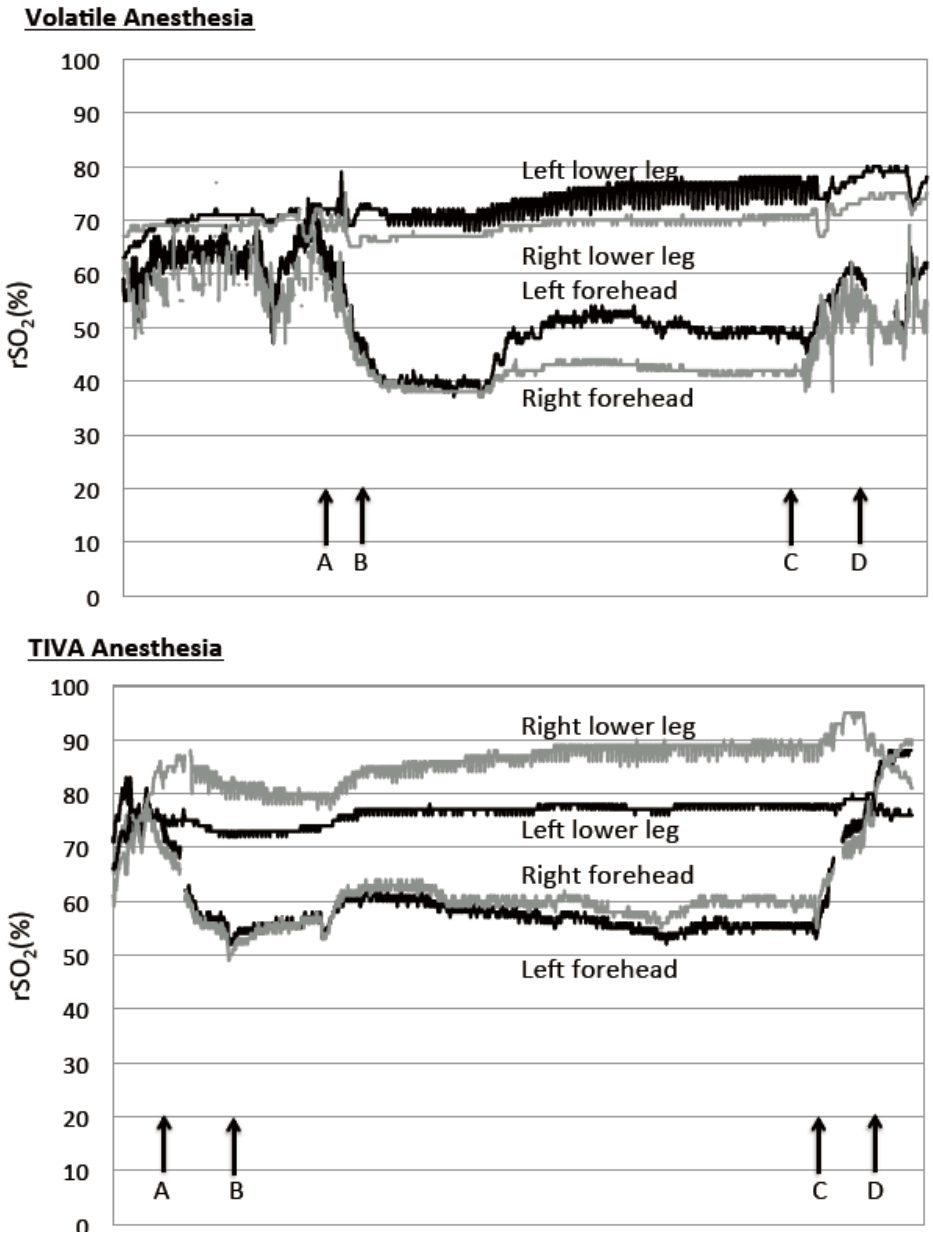

Figure 1. Changes of rSO_2 in beach-chair (BC) position

A: placing the patient in BC position B: BC position achieved

C: end of operation D: return to supine position

Nonopioid Cannabinoid Type 2 Receptor Agonist (MDA7) Prevents Paclitaxel-Induced Central Sensitization and Mechanical Allodynia

Authors: Jiang Wu, Mark Hocevar, Bihua Bie, Joseph F. Foss, Mohamed Naguib

Introduction: Paclitaxel-induced neuropathy is associated with morphologic and biochemical alterations in dorsal root ganglia satellite cells, hyperplasia/hypertrophy of macrophages in the peripheral nervous system, and microglial and astrocyte activation within the spinal cord. This neuroinflammatory process causes central sensitization, leading to the persistent pain states. There is, therefore, a critical need to determine how paclitaxel alters pain sensation due to microglial activation and central sensitization. Cannabinoid receptor type 2 (CB2) is expressed primarily in the immune system including microglia in the CNS. MDA7 is a novel selective CB2 agonist that has shown efficacy in ameliorating microglial activation and preventing allodynia in rodent models of neuropathic pain. The central hypothesis is that paclitaxel triggers the expression of microglial P2X4 receptor in the dorsal horn. The influx of Ca^{2+} *via* P2X4 receptors enhances the activity of Ca^{2+}/calmodulin-dependent protein kinase II (CaMKII) and transcriptional factor cyclic AMP response element binding protein (CREB), which subsequently increase ΔFosB expression and induces upregulation of microglial BDNF. The release of BDNF from microglia facilitates glutamatergic transmission and suppresses GABAergic transmission in dorsal horn neurons, contributing to paclitaxel-induced neuropathic pain. Since CB2 receptors are expressed on activated microglia, it is further hypothesized that the CB2 receptor functions in a negative-feedback loop and that early administration of a CB2 agonist can suppress the mechanism underlying the spinal microglial activation and BDNF upregulation, thus mitigating the central sensitization and pain behavior induced by paclitaxel.

Methods: Rats received 1.0 mg/kg i.p. of paclitaxel (or vehicle) daily for 4 consecutive days. MDA7 (15 mg/kg) or vehicle was injected (i.p.) 15 min before the administration of paclitaxel for 4 days and continued for another 10 days (a total of 14 days). AM630 (5 mg/kg i.p.), a selective CB2 receptor antagonist, was used in subsets of experiments. Mechanical sensitivity was assessed by using a series of Von Frey filaments with logarithmic incremental stiffness. Immunostaining and immunoblotting were performed to examine the activation state of microglia and the expression of BDNF and other proteins in dorsal horn (L4-5).

Results: Administration of paclitaxel resulted in tactile allodynia in rodent models (**Fig. 1**), which was alleviated by MDA7 treatment (**Fig. 1**). Because MDA7 is a specific CB2 agonist, it shows efficacy in treating mechanical allodynia in $CB2^{+/+}$, but not $CB2^{-/-}$ mice (**Fig. 1B,C**).

Paclitaxel significantly increased microglia activity (**Fig. 2A**) and CB2 expression (**Fig. 2B**) in the dorsal horn, which was attenuated by MDA7. Paclitaxel induced microglia polarization as shown by increased expression of IL-6 (M1 marker) (**Fig. 3A,B**) in the dorsal horn, which was attenuated by MDA7. In addition, MDA7 treatment was associated with increased expression of IL-10 (M2 marker) in the dorsal horn (**Fig 3. C**) and prevented the upregulation of microglial P2X4 in paclitaxel-treated rats (**Fig. 4**).

Paclitaxel also substantially increased the expression of CaMKIIα, phosphorylated CREB, ΔFosB and BDNF in the dorsal horn (L4-L5) tissue in rats treated with paclitaxel, which was reversed by MDA7 (**Fig. 5**). Furthermore, paclitaxel significantly increased the expression of glutamate receptor subunits NR2B and GluR1, and decreased expression of anion transporter KCC2 in the dorsal horn, which was reversed by MDA7 (**Fig. 6**).

Conclusion: Paclitaxel induced mechanical allodynia, microglial polarization, BDNF upregulation, and central sensitization in dorsal horn in the rats, which was prevented by MDA7. This study clarifies the spinal mechanism of paclitaxel-induced neuropathic pain and its modulation by a selective CB2 agonist, MDA7, which will ultimately lead to the development of effective approach to treat or prevent chemotherapy-induced neuropathy.

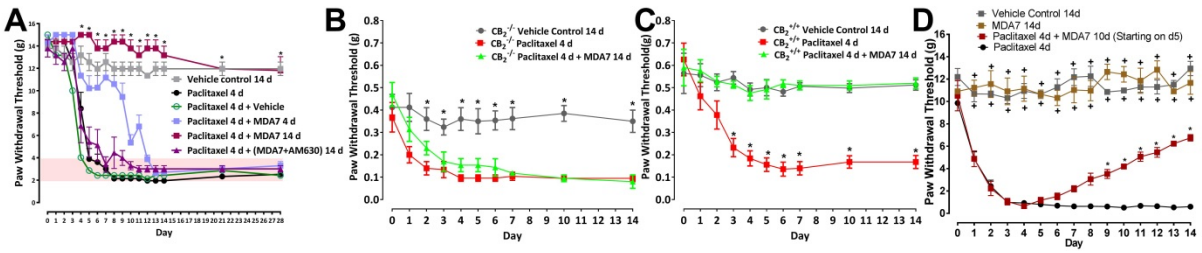

Fig. 1 MDA7 prevented paclitaxel-induced mechanical allodynia in rats (**A**) and $CB2^{+}/^{+}$ **(B)** but not $CB2^{-}/^{-}$ mice **(C)**. Significantly decreased paw withdrawal threshold was observed in the rats (n = 6 in all groups except vehicle control, n = 4) and $CB2^{+}/^{+}$ (n = 5), but not $CB2^{-}/^{-}$ (n = 5), mice injected with paclitaxel (1 mg/kg, day 1 to day 4). This was significantly extended by MDA7 (15 mg/kg, day 1 to day 14). **(D)** Treatment with MDA7 (15 mg/kg, day 5 to day 14) after the establishment of allodynia also significantly attenuated the mechanical hypersensitivity in the rats injected with paclitaxel (n = 6). $^{*,+}P < 0.01$ compared with other groups (linear mixed model with treatment and day effects with repeated measures over days).

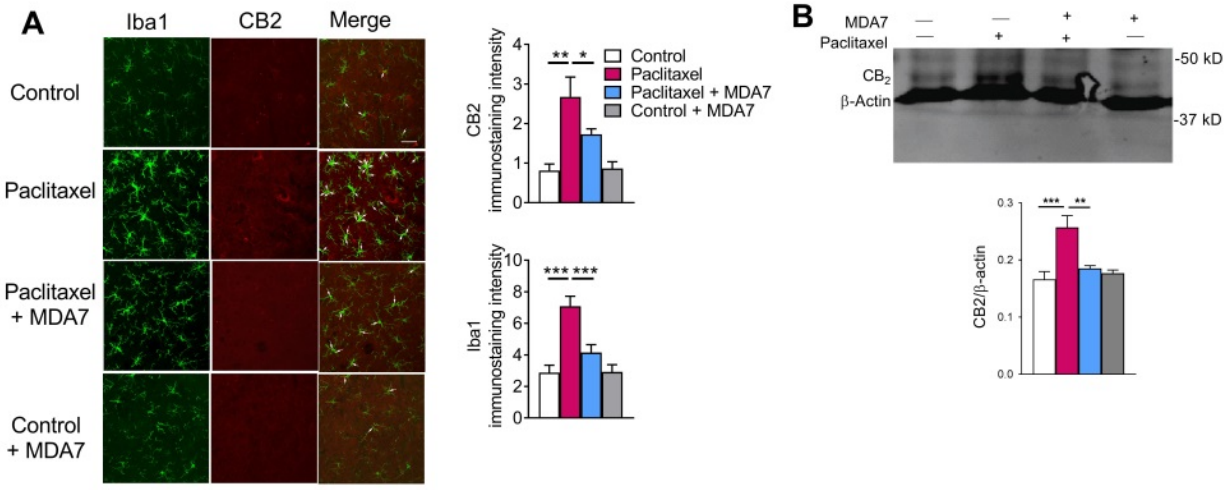

Fig. 2. Paclitaxel increased microglia activity and CB2 expression in the dorsal horn, which was attenuated by MDA7. (**A**) Increased microglia complexity and Iba1 (green) intensity was observed in dorsal horn in rats treated with paclitaxel, which was attenuated by MDA7. (**B**) The increased immunosignal of CB2 receptor in microglia was also observed in the dorsal horn of rats presented with allodynia after paclitaxel treatment. This effect was modulated by MDA7 (n = 6-7 per group). Scale Bar = 100 μm. *P<0.05; **P<0.01; ***P<0.001. Tissues were obtained on day 15 from animals described in Fig.1D.

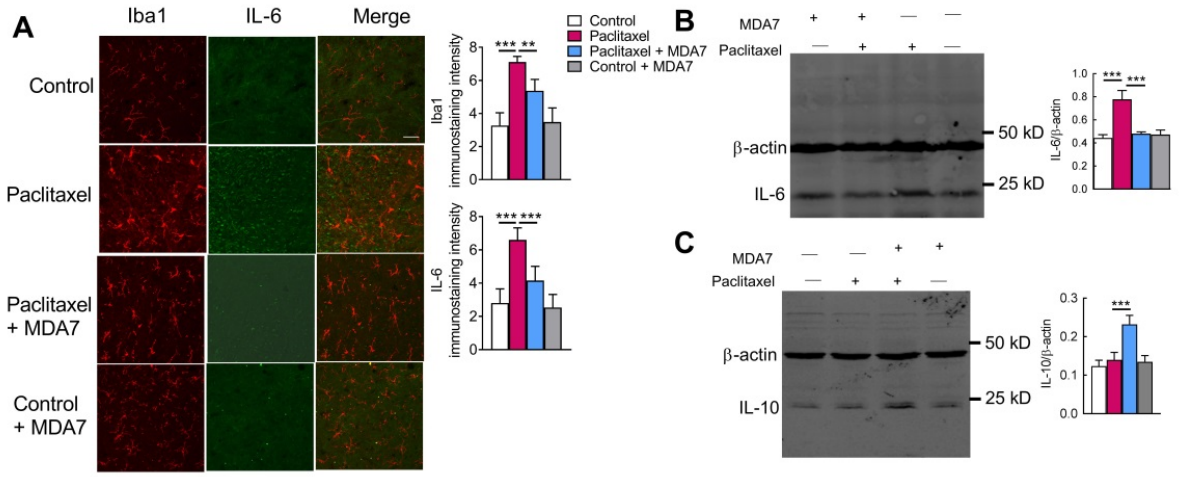

Fig. 3. Paclitaxel induced microglia polarization that was modulated by MDA7. (A) Increased expression of IL-6 (M1 marker) in microglia was observed in dorsal horn in rats treated with paclitaxel, which was attenuated by MDA7. (**B**) The increased immunosignal of IL-6 (M1 marker) in the microglia in the dorsal horn was attenuated by MDA7. (**C**) Treatment with MDA7 also increased the expression of IL-10 (M2 marker) in the dorsal horn of rats injected with paclitaxel (n = 6-7 per group). ***P<0.001. Scale Bar = 50μm.

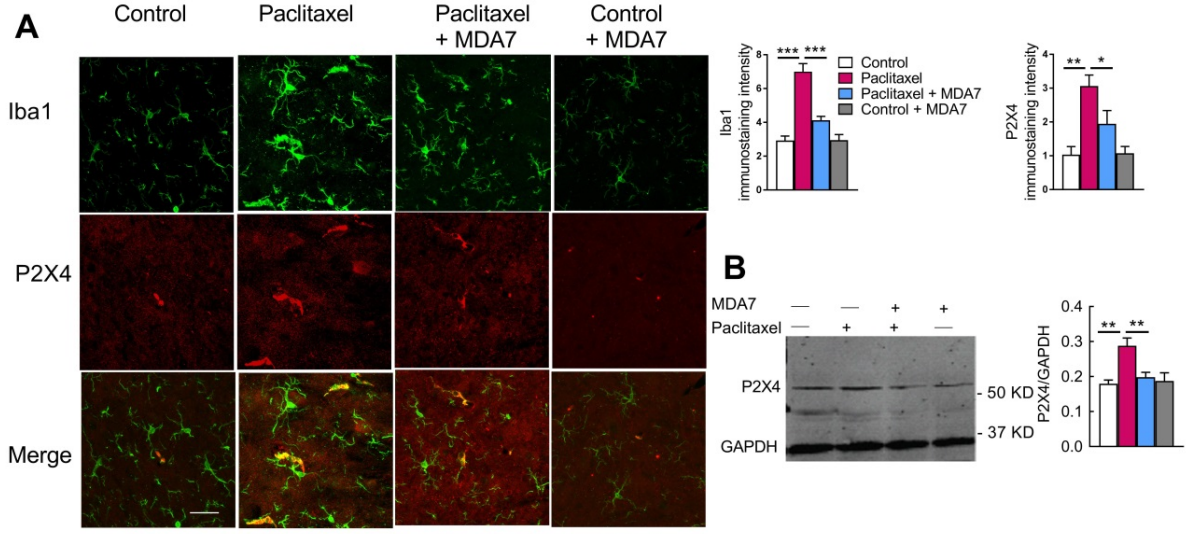

Fig. 4. Paclitaxel increased the expression of P2X4 in the microglia (A, n = 5) in the dorsal horn, which was attenuated by MDA7. (**B**) Immunoblotting study also found an increased P2X4 in dorsal horn, which was decreased by MDA7 (n = 6-7). Scale bar = 100 μm. *, P<0.05; **, P<0.01, ***, P<0.001.

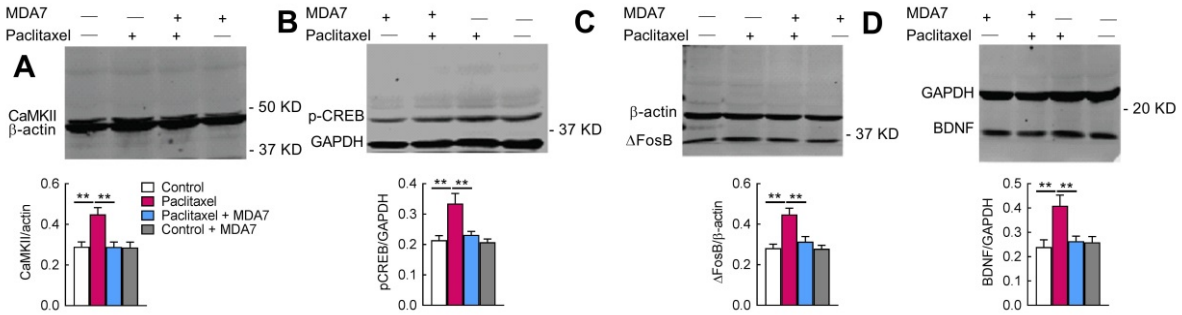

Fig. 5. Paclitaxel increased the expression of CaMKII (A), p-CREB (B), ΔFosB (C) and BDNF (D) in the dorsal horn in rats, which was attenuated by MDA7. **, P<0.01, n = 6-7 per group.

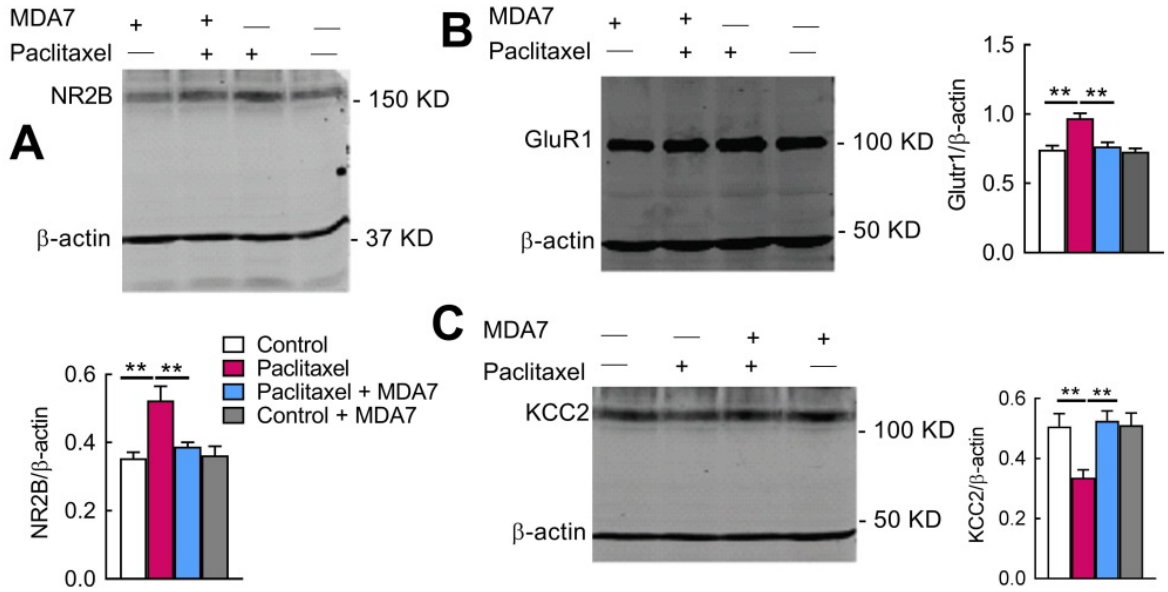

Fig. 6. Paclitaxel significantly increased the expression of glutamate receptor subunits NR2B (A) and GluR1 (B), and decreased expression of anion transporter KCC2 (C) in the dorsal horn in rats, which was reversed by MDA7. **, P<0.01, n = 6-7 per group.

Reduction of Astrocytic Glutamate Transporter Contributes to Amyloid-Induced Microglial Pruning of Synapses

Authors: Jiang Wu, Mark Hocevar, Joseph F. Foss, Bihua Bie, Mohamed Naguib

Introduction: Astrocytes are the most abundant and heterogeneous type of glial cells in the brain. To determine how dysfunctional astrocyte glutamate transporters contribute to microglial pruning of glutamatergic synapses and memory deficiency induced by amyloid fibrils, we tested the hypothesis that amyloid fibrils impair astrocyte glutamate transporters, thus leading to an abnormal accumulation of extrasynaptic glutamate, which in turn contributes to microglial pruning of glutamatergic synapses and memory deficiency in the rodent models of Alzheimer's disease (AD).

Method: $A\beta_{1\text{-}40}$ fibrils were microinjected bilaterally into hippocampal CA1 areas in rats. In another cohorts, DL-threo-beta-benzyloxyaspartate (DL-TBOA), a specific inhibitor of glutamate transporter 1 (GLT1), or ceftriaxone (used to enhance GLT1 function) were also microinjected into hippocampal CA1 areas. Immunostaining and immunoblotting were performed to detect the expression of GLT1 in astrocytes. Complement C1q production and microglial pruning of glutamatergic synapses were assessed by 3D immunofluorescence imaging. Morris water maze test was performed to evaluate the cognitive function.

Results: We first noted a significant GLT1 reduction in the hippocampal astrocytes in rats injected with amyloid fibrils, indicating dysfunctional glutamate uptake (**Fig. 1**). Microinjection of ceftriaxone significantly attenuated C1q expression and endocytosis of vGluT1 within microglia, and improved behavioral performance in the modeled rats (**Fig. 2**). These results suggested that upregulation of GluT1 expression restored the synaptic microglial pruning and cognition impaired by amyloid fibrils. Meanwhile, in naïve rats, microinjection of 10 nmol of DL-TBOA substantially increased C1q expression, increased localization of vGluT1 within microglia, and impaired performance in the Morris water maze (**Fig. 3**). This suggests that dysfunctional GluT1, which likely leads to extracellular accumulation of glutamate, contributes to C1q-mediated microglial pruning of synapses and cognitive deficits induced by amyloid fibrils.

Conclusion: The present study demonstrates that reduction of astrocytic GLT1 contributes to C1q production and microglial pruning of glutamatergic synapses, hippocampal synaptic dysfunction and memory deficit in the rodent AD model. Our data highlight new aspects in our understanding of the pathogenesis of AD, and provides new approaches for identification and development of novel therapeutic targets for AD.

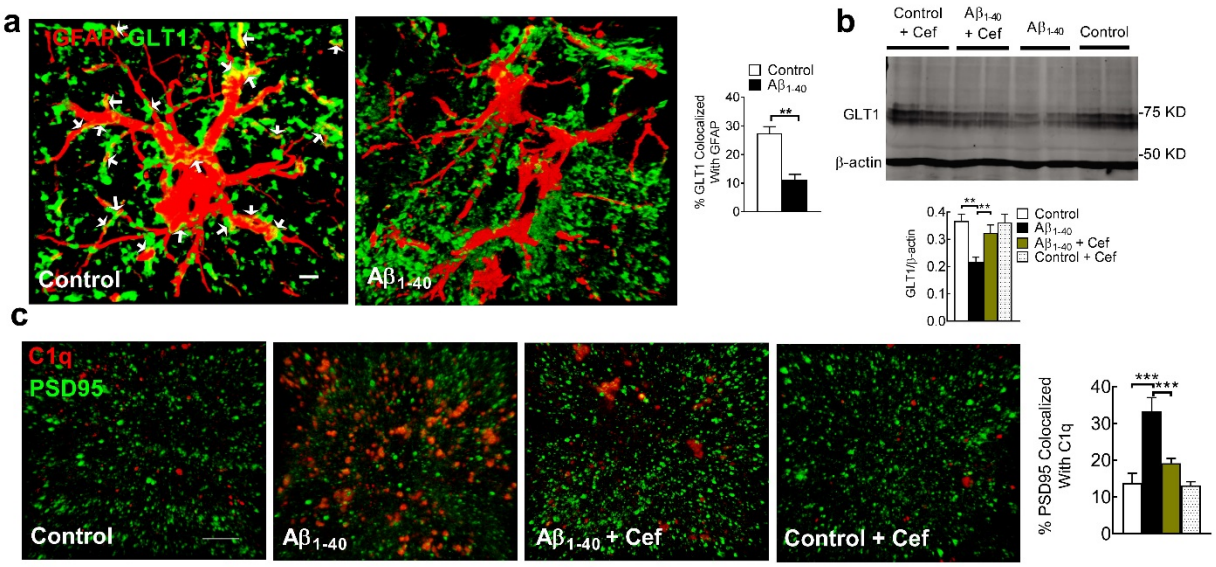

Fig. 1. Enhancement of astrocytic GLT1 function attenuated the C1q-mediated microglial pruning of synapses. Significantly decreased expression of GLT1 was observed in hippocampal CA1 in the modeled rats (***a,*** n = 7), which was recovered by microinjection of ceftriaxone (0.1 mg×7 days, ***b***, n=7); (***c***) Ceftriaxone also decreased the hippocampal C1q expression in astrocytes (***c,*** n = 6-7). The solid arrow indicated the internalization of vGluT1 within the microglia (Iba1), and the open arrow showed the overlay, not the internalization, of the immunosignals of Iba1 and vGluT1. **P<0.01; ***P<0.001. Data represent mean ± s.e.m

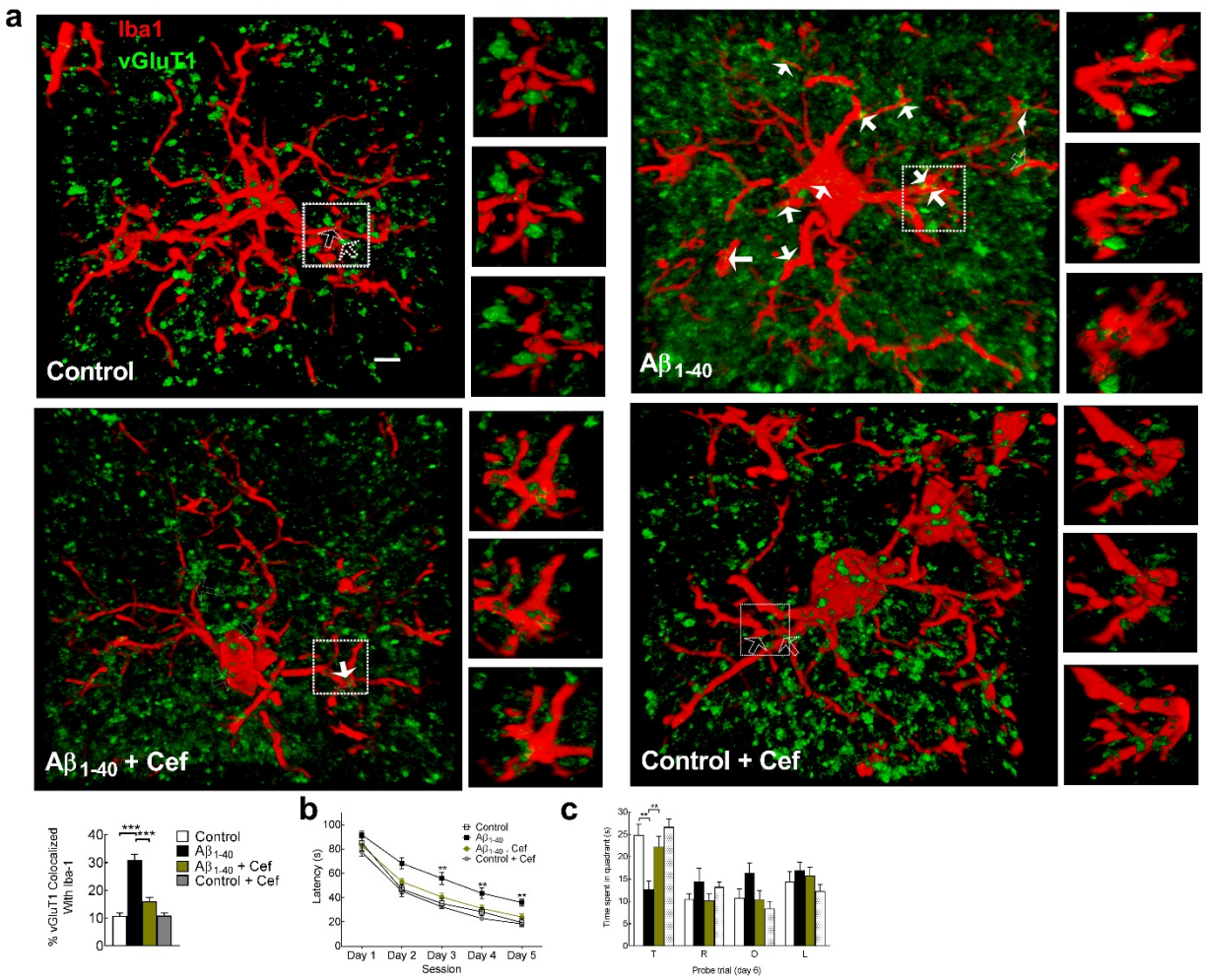

Fig. 2. Ceftriaxone decreased phagocytosis of vGluT1 by microglia (***a***, n = 4 rats; scale bar = 10 μ), decreased the escape latency (***b***) and increased the time in the target quadrant (***c***) in the modeled rats (n=10). An islet was rotated at about -45°, 0°, and 45° as described. The solid arrow indicated the internalization of vGluT1 within the microglia (Iba1), and the open arrow showed the overlay, not the internalization, of the immunosignals of Iba1 and vGluT1. **P<0.01; ***P<0.001. Data represent mean ± s.e.m.

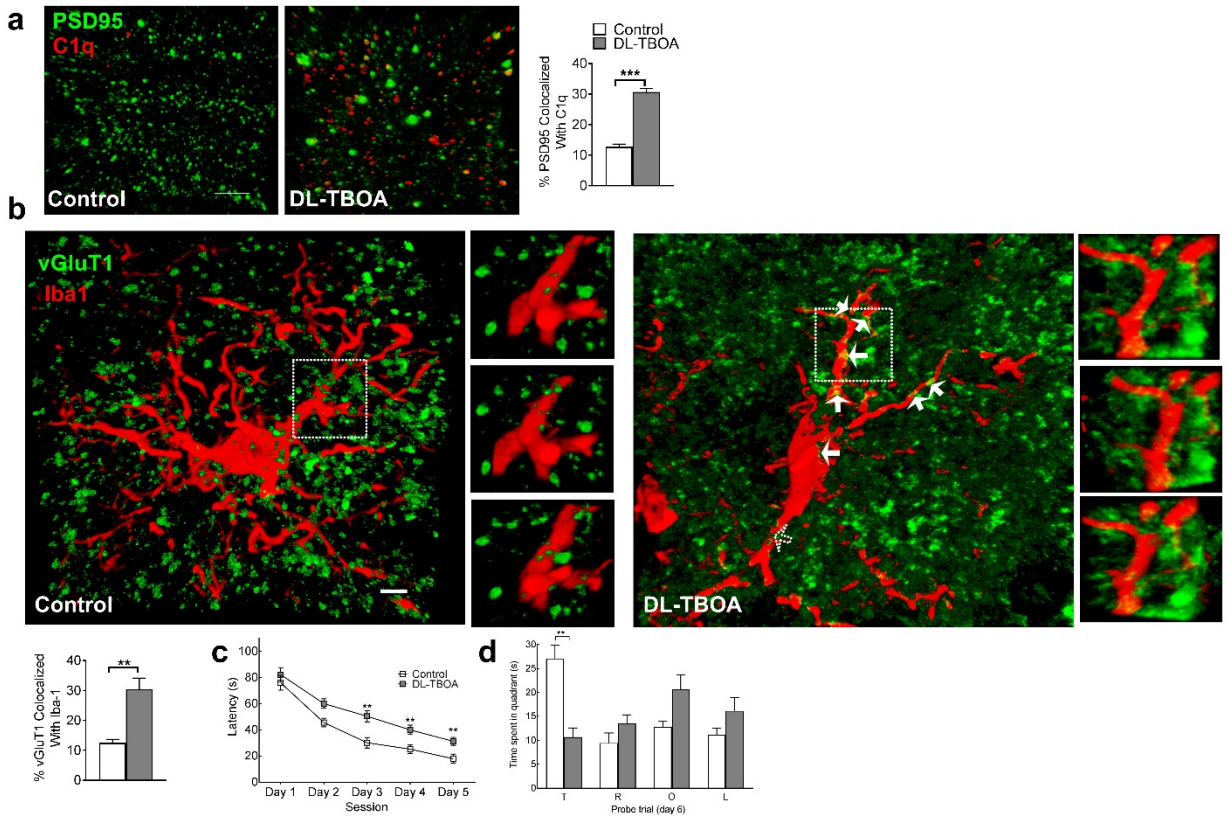

Fig 3. Suppression of astrocytic GLT1 by DL-TBOA induced microglial pruning of glutamatergic synapses. (**a**) DL-TBOA induced significant increase of C1q expression in the hippocampal CA1 synaptosome and its colocalization with PSD 95 in naïve rats (n = 4 sections from 5 rats); (***b-d***) DL-TBOA increased the phagocytosis of vGluT1 by microglia in the hippocampal CA1 (***b***, n = 4 rats per group; scale bar = 10 μ), increased escape latency (***c***, n = 10), and decreased the time in the target quadrant (***d***, n = 10) in the control rats. An islet was rotated at about -45°, 0°, and 45° as described. The solid arrow indicated the internalization of vGluT1 within the microglia (Iba1), and the open arrow showed the overlay, not the internalization, of the immunosignals of Iba1 and vGluT1. **, P<0.01; ***, P<0.001. Data represent mean ± s.e.m.

Teasing Apart the Desired Effects of Anesthetics from Unwanted Side Effects at $GABA_A$ Receptors

Authors: Noëlie S Cayla[1], Beza A Dagne[1], M Frances Davies[1], Yun Wu[1], Eric R Gross[1], M Bruce MacIver[1], Edward J Bertaccini[1,2]

1. Department of Anesthesiology, Pain and Perioperative Medicine
2. Department of Anesthesia, Palo Alto VA Health Care System

Background: GABA receptors are important molecular targets for anesthetics, but it remains unclear how these receptors are involved in producing unconsciousness or contributing to unwanted side effects. Our group has developed new anesthetic agents that specifically target $GABA_A$ slow receptors. Using *in silico* docking-based screening algorithms, a novel molecular core was designed to target the same binding site as etomidate and propofol. Structures were designed to eliminate etomidate's side effect causing adrenal suppression. A series of compounds was generated by the program and the top ten compounds were first tested on tadpoles, then in rat brain slice electrophysiology experiments. Finally, *in vivo* experiments were conducted with propofol and the most promising experimental drug of the series, BB, to compare their hemodynamic effects.

Methods: For the *in vivo* studies, the compounds where pipetted into the amphibians' water and rats were administrated drugs by intravenous bolus. For electrophysiology, rat brain slices were incubated for at least two hours prior to experiment, and submerged in artificial cerebrospinal fluid (ACSF). In the hippocampal CA1 area, bipolar tungsten stimulating electrodes were placed to evoke field potentials via Schaffer-collateral fiber inputs. Paired-pulse population spike (PS) responses were recorded using a microelectrode placed near the pyramidal cell body. Control recordings were acquired with brain slices before and after a test compound was added to the ACSF. Additionally, we compared the experimental compound's actions with those produced by propofol and etomidate, agents known to selectively increase $GABA_AR$-mediated inhibition. We used picrotoxin, a chloride channel blocker to probe $GABA_AR$ involvement in effects.

Results: When exposed to BB, tadpoles quickly lost consciousness then fully recovered. When BB was injected into rats, the rodents also lost consciousness and recovered fully. Also, their heart rate and blood pressure were considerably more stable compared to propofol effects. Our electrophysiology results show that etomidate and BB produced a reversible enhancement of GABAAR-mediated slow inhibition that was more selective than propofol. All of BB's effects occurred by acting specifically on $GABA_A$-slow receptors, like etomidate. Propofol, in contrast, clearly enhanced other forms of $GABA_AR$-mediated inhibition (e.g. fast and tonic receptors). The effects of all agents were fully reversed by picrotoxin.

Conclusions: The experimental compound BB had an anesthetic effect via $GABA_A$Rs as predicted. It was more selective than propofol, which acted mainly on $GABA_A$-fast, followed by -tonic and slow receptors, instead of just the $GABA_A$-slow receptors that were most sensitive to our experimental compounds. Thus, both etomidate and our experimental compound BB demonstrated the same $GABA_A$R selectivity, which correlates with the observed decreased in undesirable hemodynamic side effects for both compounds compared to propofol.

Use of Methadone in Pediatric Posterior Spinal Fusion: A Randomized, Controlled Trial

Presenting Author: Lindsay Juriga[1]
Co-Authors: Arbi Ben Abdallah[1], Michael C. Montana[1], Evan D. Kharasch[1], and Anshuman Sharma[1]

[1]Washington University in St. Louis Department of Anesthesiology, St. Louis, MO.

Background/Introduction: Patients undergoing major spine surgery experience severe pain postoperatively, require large amounts of opioids, and frequently have adverse respiratory events. Methadone is a μ-opioid agonist with slow elimination, resulting in prolonged effects, and may significantly diminish the need for postoperative analgesics. It has no active metabolites or pro-drug forms, and is metabolized by cytochrome P450 2B6. We previously demonstrated that methadone (0.1-0.3 mg/kg) follows linear pharmacokinetics in adolescents. In this follow up study, we aimed to assess a) if a single dose of intraoperative methadone, when used as the sole intraoperative opioid, can lead to a reduction in opioid consumption; and b) assess the pharmacokinetics of a dose of 0.4 mg/kg of methadone in pediatric patients.

Methods: After IRB approval, patients were consented on the day of surgery. Based on the results of our previous study, subjects were randomized 1:2 to either control (intraoperative opioid per anesthesiologist discretion) or methadone HCl (0.4 mg/kg ideal body weight). After unexpectedly observing sedation in the subjects receiving 0.4 mg/kg methadone, a decision was made to reevaluate the effects of the 0.3 mg/kg dose. Subjects in this cohort were randomized 1:2 to receive either control or 0.3 mg/kg methadone. Anesthesia and surgical care was not altered for the purpose of this investigation. To examine pharmacokinetics, blood samples were drawn at 0, 5, 30, 60, 90, 120, 180, 240, 360, 480, 600, and 720 minutes following methadone administration, and every morning for up to six days post-operatively, or until hospital discharge. We compared total opioid consumption in morphine equivalents, pharmacokinetic data, postoperative pain scores, and adverse events between the groups.

Results: Patients were between 11 to 18 years old. Twenty patients received 0.3 mg/kg methadone, 13 received 0.4 mg/kg, and 15 did not receive methadone. Total hospital stay opioid consumption in IV morphine equivalents was compared between the three groups. One-way, between subjects ANOVA demonstrated a significant difference between the groups [$F(2, 45) = 3.88$, $p = 0.0279$]. Post hoc comparisons using Tukey's test demonstrated a significant difference between the control group (3.34 ± 0.93 mg/kg) and the 0.3 mg/kg methadone group (2.51 ± 0.84 mg/kg). There was no difference between the 0.4 mg/kg methadone group (2.77 ± 0.90 mg/kg) and either the control or the 0.3 mg/kg methadone groups. There was no significant difference in average daily pain scores between the groups. Patients administered 0.4 mg/kg methadone had peak plasma concentration of 176 ± 104 and 231 ± 132 ng/ml R- and S-

methadone respectively. Peak plasma R- and S methadone was respectively 99 ± 37 and 129 ± 44 ng/ml in patients given 0.3 mg/kg methadone. Preliminary analysis of adverse events (e.g. respiratory depression, excessive sedation, decreased oxygen saturation, reintubation, or altered mental status) suggest similar frequencies of these events between the three groups.

Conclusions: The use of a single dose of intraoperative methadone is associated with a significant decrease in overall opioid consumption without a change in average daily pain scores following posterior spinal fusion surgery in adolescents. Retrospective examination of this study and our previous study suggest the unexpected sedation seen with the 0.4 mg/kg methadone dose may be due to the institution of a post-operative pain treatment protocol that includes gabapentin and methocarbamol.

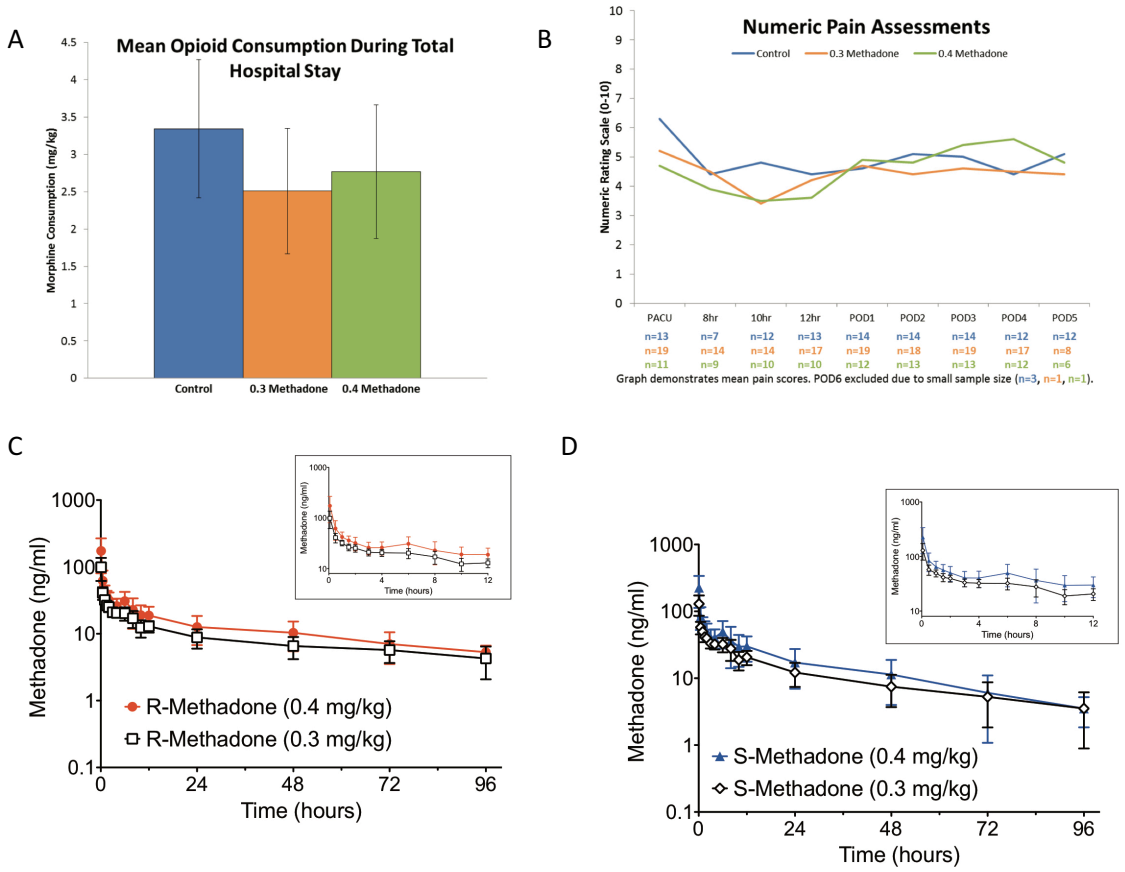

Figure Legend: a) Total hospital stay opioid consumption in IV morphine equivalents; b) PACU, 8, 10, 12 hours postoperative, and average daily pain scores; c) and d) R- and S-methadone pharmacokinetics over 96 hours with 0 to 12 hours post IV bolus dosing presented as insets.